Climate teleconnections influence on West Africa's terrestrial water storage

Christopher E. Ndehedehe[a,c], Joseph L. Awange[a,b], Michael Kuhn[a], Nathan O. Agutu[a,d], and Yoichi Fukuda[b]

[a]*Department of Spatial Sciences, Curtin University, Perth, Western Australia, Australia.*
[b]*Department of Geophysics, Kyoto University, Japan*
[c]*Department of Geoinformatics and Surveying, University of Uyo, P.M.B. 1017, Uyo, Nigeria.*
[d]*Department of Geomatic Engineering and Geospatial Information Systems JKUAT, Nairobi, Kenya.*

Abstract

There is some evidence of rapid changes in the global atmosphere and hydrological cycle caused by the influence of climate variability. In West Africa, such changes impacts directly on water resources leading to incessant extreme hydro-meteorological conditions. This study examines the association of three global climate teleconnections (El-Niño Southern Oscillation (ENSO), Indian Ocean Dipole (IOD), and Atlantic Multi-decadal Oscillation (AMO)) with changes in terrestrial water storage (TWS) derived from both Modern-Era Retrospective Analysis for Research and Applications (MERRA, $1980-2015$) and Gravity Recovery and Climate Experiment (GRACE, $2002-2014$). In the Sahel region, positive phase of AMO coincided with above-normal rainfall (wet conditions) and the negative phase with drought conditions, and confirms the observed statistically significant association ($r = 0.62$) between AMO and the temporal evolutions of standardised precipitation index. This relationship corroborates the observed presence of AMO-driven TWS in much of the Sahel region (though considerably weak in some areas). While ENSO appears to be more associated with GRACE-derived TWS over the Volta basin ($r = -0.40$), this study also shows a strong presence of AMO and ENSO induced TWS derived from MERRA reanalysis data in the coastal West African countries and most of the regions below latitude 10°N. The observed presence of ENSO and AMO driven TWS are noticeable in tropical areas with relatively high annual/bimodal rainfall and strong inter-annual variations in surface water. The AMO has a wider footprint and sphere of influence on the region's TWS and suggests the important role of North Atlantic Ocean. IOD related TWS also exists in West Africa and its influence on the region's hydrology maybe secondary and somewhat complementary. Nonetheless, presumptive evidence from the study indicates that ENSO and AMO are the two major climatic indices more likely to impact on West Africa's TWS.

Keywords: Rainfall, ENSO, Climate Variability, Droughts, West Africa, SPI

1. Introduction

Extreme climatic conditions (e.g., droughts and floods) in West African countries (Fig. 1) caused by large-scale ocean-land-atmospheric interactions and global climate teleconnections (e.g., El-Niño Southern Oscillation-ENSO) represent considerable impact on annual and seasonal variability in freshwater. Drying trends and deficits in precipitation, soil moisture, and net precipitation flux, for instance, as observed in the region have been linked to warming of the tropical oceans, anthropogenic emissions of aerosols and greenhouse gases, and other processes of oceanic inter-annual variations (e.g., Andam-Akorful et al., 2017; Nicholson, 2013; Oguntunde and Abiodun, 2013; Sheffield and Wood, 2008; Giannini et al., 2008). These trends, which are also driven and influenced by competing multiple physical mechanisms (Druyan, 2011), might impact substantially, either directly or indirectly on terrestrial water storage (TWS; total of surface waters (i.e., rivers, lakes, and wetlands), soil moisture, canopy storage, and groundwater) in the region.

The global atmosphere and hydrological cycle are undergoing rapid changes driven by the influence of climate variability and teleconnections (see, e.g., Phillips et al., 2012; Hurkmans et al., 2009; Malhi and Wright, 2004). Variability in ENSO amongst other factors (e.g., rainfall, temperature, barometric pressure, etc.), for example, was associated with changes in aquifer water levels in Japan (see, Dong et al., 2015). In Africa, climate variability at decadal to century scales resulted in recharge rates of 30 mm/yr (see, Scanlon et al., 2006). Trans-Niño index showed strong association with stream flow during the warm phase of Pacific Decadal Oscillation (PDO) in the Upper Klamath Lake in the US (see, Kennedy et al., 2009) whereas more recently, a low frequency modulating El-Niño activity was found to have induced lower changes in rainfall variance over West Africa (see, Andam-Akorful et al., 2017). Obviously, the observed extremes in West African rainfall (especially the Guinea Coast) is likely to increase owing to the strong impacts of climate variability, environmental changes, influence of tropical Atlantic sea surface temperature (SST) anomalies, and the nature of West African Monsoon, which is largely controlled by interactions between continental surfaces and the oceans (see, e.g., Rodríguez-Fonseca et al., 2011; Losada et al., 2010; Redelsperger and Lebel, 2009; Polo et al., 2008; Redelsperger et al., 2006). The overarching outcomes of a plethora of related studies in West Africa (see, e.g., Ndehedehe et al., 2016c; Diatta and Fink, 2014; Nicholson, 2013; Paeth et al., 2012; Bader and Latif, 2011; Joly and Voldoire, 2010; Losada et al., 2010; Ali and Lebel, 2009; Giannini et al., 2008; Reason and Rouault, 2006), be it region-specific or basin scale, overwhelmingly agree on the roles of climatic variations through changes in the global oceans, mesoscale convective systems, and indices of climate variability (e.g., ENSO,

Atlantic Multi-decadal Oscillation-AMO, PDO, etc.) on precipitation patterns and other water fluxes (e.g., stream flow). Thus, climate variability is expected to significantly impact on hydrological conditions, leading to considerable impacts on changes in TWS. Such impacts amongst other factors could restrict agriculture, ecosystem services and the region's freshwater systems, warranting the study of climate teleconnections and its contributions to long term changes in TWS. Since climate teleconnections also provide significant influence on meteorological processes, and TWS being a hydrologic state variable that integrates hydrologic processes (e.g., recharge and infiltration), the knowledge of climate teleconnection's influence on TWS is critical and provides meaningful insights on drought events, wet conditions, and water resources management. Ultimately, identifying teleconnections that impact TWS in the region will be beneficial for forecasting.

The pioneering works of Phillips et al. (2012) and Boening et al. (2012) have shown how ENSO teleconnection patterns around the globe are associated with changes in global mean sea level and continental water storage derived from Gravity Recovery and Climate Experiment (GRACE, Tapley et al., 2004). Given that ENSO has large energy between 2-5 years, only a few cycles will occur in the 8-year GRACE data used by Phillips et al. (2012). On the other hand, Boening et al. (2012) did not dwell on the relationship between continental stored water and climate teleconnections, but showed that the 5 mm decline in global mean sea level (GMSL) was tied to the 2010/2011 La-Niña. This significant decrease in GMSL according to the study, caused an excess transport of freshwater from ocean to land areas. Since ENSO is mostly based on oceanic variability in the Pacific, the role of other climate indices that describes variability in the Atlantic and Indian Oceans on TWS also requires reckoning. An extended hydrological time series will provide more evidence on climate tele-connection driven changes in TWS at the regional or global scale.

Globally, observed variations in precipitation, soil moisture, freshwater discharge, recharge, and drought characteristics have been attributed to variabilities in ENSO, AMO, and PDO (e.g., Andam-Akorful et al., 2017; Dai et al., 2009; Hurkmans et al., 2009; Sheffield and Wood, 2008; Scanlon et al., 2006). Like many other parts of the world, rainfall and hydro-climatic conditions in West Africa are influenced by ENSO and a number of other global climate teleconnections (AMO, Indian Ocean Dipole-IOD, etc. see, e.g., Ndehedehe et al., 2016b,c; Diatta and Fink, 2014; Molion and Lucio, 2013; Paeth et al., 2012; Bader and Latif, 2003, 2011; Giannini et al., 2003; Nicholson et al., 2000; Nicholson, 2013, and the references therein). These climate teleconnections result in extreme hydrological conditions and intensification of the water cycle, all of which impact on TWS in the region. Although the influence of these

climate teleconnections and other climate modes on West African rainfall has been widely studied as indicated, their influence on TWS in the region has, however, not been considered. Moreover, although rainfall is the main input of TWS, the influence of teleconnections on rainfall might not directly be the same as its influence on TWS, which is a vertical integration of surface water, groundwater, soil moisture, ice/snow and biomass, all of which might respond differently to climate variability. Despite this, the few studies available over West Africa that addressed TWS (see, e.g., Ndehedehe et al., 2016a; Henry et al., 2011; Grippa et al., 2011; Hinderer et al., 2009; Forootan et al., 2014) do not consider the influence of climate teleconnections on its TWS changes.

This manuscript investigates the association of three well known global climate teleconnections (ENSO, Indian Ocean Dipole-IOD, and AMO) on the region's TWS and highlights the influence of climate teleconnection-induced rainfall on TWS. To this end, this study assumes that these teleconnection indices (Fig. 2), which directly or remotely contribute to extreme hydro-meteorological conditions (i.e., extreme wetness and dryness) in the region (see, e.g., Diatta and Fink, 2014; Paeth et al., 2012; Nicholson et al., 2000), subsequently influences TWS changes over the region. Specifically, the two main objectives of this study are (i) to identify the spatio-temporal modes of precipitation anomalies (i.e., wet and dry conditions) over two different timescales (i.e., 6 and 12 month aggregations) that influence TWS variations over West Africa, and (ii) examine the relationship of TWS derived from GRACE ($2002-2014$) and Modern-Era Retrospective Analysis for Research and Applications (MERRA, Rienecker et al., 2011) ($1980-2015$) to climate teleconnections. In trying to achieve these objectives, the present study employs for the first time a methodological framework based on multivariate analysis that allows the assessment of hydrological processes, and extreme precipitation anomalies on TWS and its association with climate teleconnections over West Africa.

To comprehensively study teleconnections' influence on TWS over West Africa, multiple-linear regression analysis (MLRA) and independent component analysis (ICA, see, e.g., Westra et al., 2010; Aires et al., 2002; Cardoso and Souloumiac, 1993; Cardoso, 1999) are combined to examine hydro-meteorological conditions and the association of climate indices with TWS derived from both GRACE ($2002-2014$) and global high-resolution MERRA data ($1980-2015$). The standardised precipitation index (SPI, McKee et al., 1993) and the ICA technique are employed to analyse the relationship of extreme hydro-meteorological conditions with these climate teleconnections.

The remainder of the study is organised as follows; in section 2, a brief highlight on the study area is provided while sections 3 and 4 provide, respectively, a discussion on the data

and methodology used. This is followed by presentation and discussion of the results in section 5. The conclusions of the study are summarized in section 6.

2. West Africa

2.1. Location

West Africa covers an areal extent of 7.5 million km^2 and comprises two major geographical zones; the countries of the Gulf of Guinea and the Sahelian countries (e.g., Amani et al., 2007; Ndehedehe et al., 2016a). The 16 member countries (Fig. 1) of this region, have an estimated population of 330 million people (USAID, 2013). The region is located between latitudes 0°N to 20°N and longitudes 20°W to 20°E excluding the highlands of Cape Verde. However, the analysis of the current study extends to the equatorial region, which includes the Congo basin (Fig. 1).

2.2. Climate and hydrology

The climate of the region consists of extreme wet and dry conditions, and the intra-annual rainfall distribution in the region is linked to seasonal migration of the intertropical convergence zone (ITCZ) and circulation features (e.g., the African Easterly Jets, Tropical Easterly Jets, African Westerly Jet)(Lebel and Ali, 2009; Nicholson, 2013; Nicholson and Grist, 2001; FAO, 1983). Rainfall varies from less than 200 mm/yr in the Sahelian countries to over 2000 mm/yr along the Gulf of Guinea. In the Gulf of Guinea region, the rainfall seasons occur between April-June and July-September, with the wettest months being June and September or sometimes October, while in the Sahel region, rainfall mostly occur between June and September, with maximum rainfall occurring in August (Nicholson et al., 2000). ENSO and AMO are well known climate teleconnections that have been associated with extreme rainfall variability in the region (see, e.g., Diatta and Fink, 2014; Paeth et al., 2012; Nicholson et al., 2000). That said, the severe droughts of the 1980's was perceived as the combined effects of unusual warming in the Indian Ocean and the eastern equatorial Atlantic Ocean (see, e.g., Bader and Latif, 2011; Giannini et al., 2003). Temperature varies with altitude, with lowland areas having a mean annual temperature above 18°C while in the Central Sahel, temperatures in July could be as high as 58°C, differing from the the southern part of the Sahara where mean monthly temperatures could rise to 30°C (FAO, 1983).

Numerous rivers such as the Niger, Benue, Volta (Black and White Volta rivers), Senegal, Oti, Comoe, and Gambia amongst others drain the West African region (Fig. 1) while the Congo river is the second largest river in Africa and drains one of the largest tropical forests of

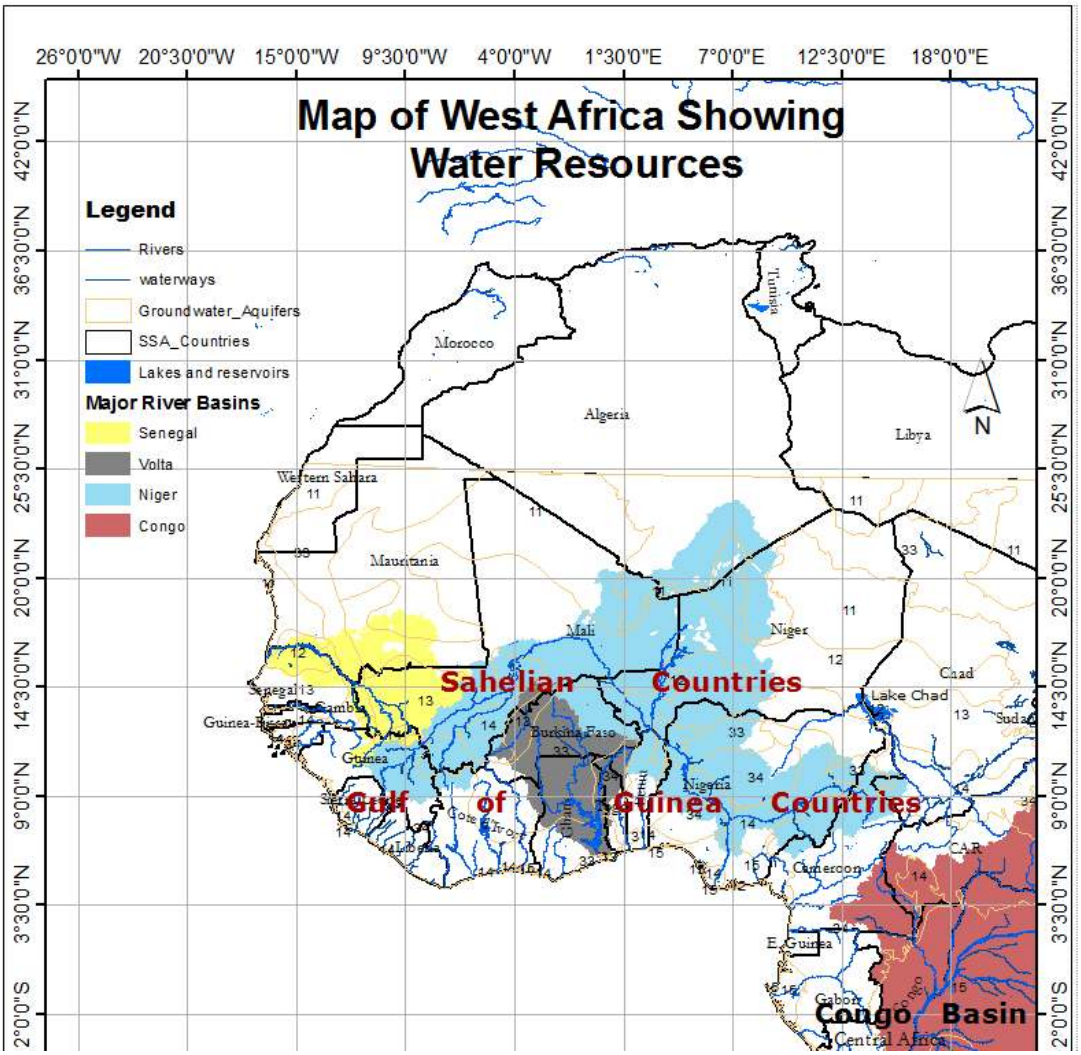

Figure 1: Study area showing countries in West Africa and some parts of Equatorial Africa (i.e., the Congo basin). Major river basins (e.g., Niger, Volta, Congo, and Senegal), rivers, lakes, and groundwater aquifers are also indicated. The Congo (tulip pink) and Niger (sky blue) river basins are considerably large and apparently the most significant and prominent basins in the region owing to the two major rivers (Niger and Congo) that provide numerous ecosystem services. The types of aquifers are described in terms of numbers; for example, the numbers ranging from 11-15 are found in major groundwater basins while the numbers 33 and 34 on the map, are those found in local and shallow aquifers. Aquifer maps and some river distribution networks were adapted from the World-wide Hydrogeological Mapping and Assessment Programme (WHYMAP) (https://www.whymap.org/whymap/EN/Downloads/Global_maps/globalmaps_node_en.html).

the world, i.e., in the Congo basin (e.g., Shahin, 2008). The aforementioned rivers are mostly shared by four and up to eight riparian countries, which sometimes results in trans-boundary water conflicts. The Niger river in particular is the longest river in West Africa and is shared by several riparian countries in the region. The Fouta Djallon Highlands where the river Niger originates from is the water tower of West Africa and shows the strongest amplitudes of TWS and precipitation over the region (see, Ndehedehe et al., 2016a). TWS and stream

flows are largely precipitation-driven with time lags in some areas. However, diversity in local climates, soil infiltration characteristics, and multiple strings of anthropogenic factors, e.g., land use change, dam constructions, and developments of small-scale reservoir systems for water mobilization to support agriculture, have also contributed to changes in hydrological regimes of water fluxes in the region (e.g., Ndehedehe et al., 2017, 2016a; Ahmed et al., 2014; Descroix et al., 2009; Favreau et al., 2009; Li et al., 2007).

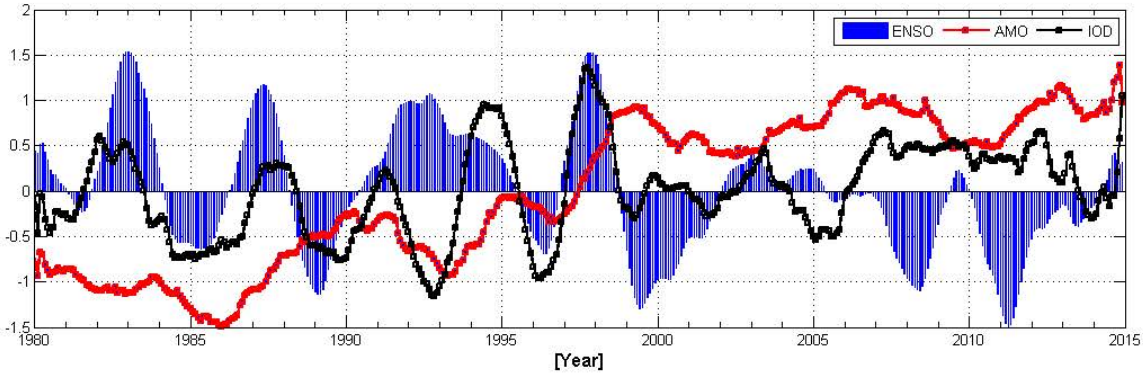

Figure 2: Time series of monthly climate indices (ENSO, IOD, and AMO) for the period of $1980 - 2014$ used in the study.

3. Data

All datasets used in this study are described below and key parameters are summarized in Table 1.

3.1. Terrestrial Water Storage (TWS)

i Gravity Recovery and Climate Experiment TWS

Since the inception of Gravity Recovery and Climate Experiment (GRACE, Tapley et al., 2004) in 2002, monthly estimates of Earth's gravity field have been used to infer changes in mass at and below the Earth's surface (e.g., Wahr et al., 1998). The Earth's water storage changes derived from GRACE observations both at basin and continental scales with global and regional applications in droughts, hydrology, climate, and validation of hydrological models have been widely studied (see, e.g., Wouters et al., 2014, and the references therein). The GRACE Release-05 (RL05) spherical harmonic coefficients from Center for Space Research (CSR) for the period 2002 to 2014 (http://icgem.gfz-potsdam.de/ICGEM/shms/monthly/csr-rl05/) are used in this study to compute changes in TWS. Since GRACE does not provide changes in degree 1 coefficients (i.e., C_{10}, C_{11}, and S_{11}) coupled with the effect of large tide-like aliases (e.g., Seo et al., 2008) in degree

Table 1: Summary of precipitation, TWS products, and teleconnection indices used in this study.

Data	Type	Period	Spatial Res.	Temporal Res.	Coverage
GPCP	Guage and satellite	1979 – 2014	2.5° x 2.5°	Monthly	Global
MERRA	Global reanalysis	1980 – 2015	0.625° x 0.5°	Monthly	Global
GRACE	Satellite gravity	2002 – 2014	1.0° x 1.0°	Monthly	Global
MEI	climate index	1980 – 2015	––	Monthly	
IOD	climate index	1980 – 2015	––	Monthly	
AMO	climate index	1980 – 2015	––	Monthly	

2 coefficients, we replace degree 1 coefficients with estimates from satellite laser ranging (Swenson et al., 2008), and following Chen and Wilson (2008), degree 2 coefficients are also replaced by those provided by Cheng et al. (2013). DDK2 decorrelation filter (Kusche et al., 2009) is then applied on the spherical harmonic coefficients in order to reduce the effect of the correlated noise. The DDK2-filtered monthly GRACE solutions are then converted to equivalent water heights on a 1° x 1° grid following the approach of Wahr et al. (1998). Monthly changes in TWS solutions $\mathbf{W}(\theta, \lambda, t)$, in time t (where θ, λ are the geographical latitudes and longitudes, respectively), after removing the long term mean $w(\lambda, \theta)$ over the investigated period are given as (Phillips et al., 2012):

$$\mathbf{X}_{TWS}(\theta, \lambda, t) = \mathbf{W}(\theta, \lambda, t) - w(\theta, \lambda). \tag{1}$$

ii Modern-Era Retrospective Analysis for Research and Applications (MERRA) TWS

One of the main purposes of the MERRA data was to improve upon the water cycle represented in previous generations of reanalyses (Rienecker et al., 2011). The data is a state-of-the-art reanalysis that provides atmospheric fields, water fluxes, and global estimates of soil moisture (Reichle et al., 2011). Also, it has been improved significantly when compared to previous reanalysis datasets (Rienecker et al., 2011). MERRA outputs have been used in the study of atmospheric circulations and assessing agricultural droughts in the African continent (see, Agutu et al., 2017; Wu et al., 2013) and has been recommended for land surface hydrological studies (Reichle et al., 2011). The land TWS data component of MERRA used in this study, covers the period of 1980 – 2015, and is available for download through the National Aeronautic and Space Administration (NASA) data portal (http://disc.sci.gsfc.nasa.gov/mdisc/). The MERRA-TWS is employed to highlight the influence of climate teleconnections on long term terrestrial stored water, complementing the limited GRACE-TWS data record.

3.2. Global Precipitation Climatology Project (GPCP)

The global grids of monthly estimate of Global Precipitation Climatology Project (GPCP) data set from 1979 – 2014 (Huffman et al., 2009; Adler et al., 2003) is used in this study. The GPCP data is a merged satellite-based product that is adjusted using rain gauge data and can be downloaded through the World Data Center website (see http:// lwf.ncdc.noaa.gov/oa/wmo /wdcamet-ncdc.html). Previous studies (see, e.g., Ndehedehe et al., 2016b; Paeth et al., 2012; Yin et al., 2004) have shown that the GPCP version 2 precipitation data has a relatively good correlation with rain gauge observations, Tropical Rainfall Measuring Mission based precipitation, and Climate Prediction Center Merged Analysis (CMAP) data. Because of its long term record and availability, the GPCP data is used here to compute standardised precipitation index (SPI) over West Africa at 6 and 12 months aggregation. Our assumption is that 6 and 12 month SPI cumulations provide a reasonable lag for extreme rainfall conditions to be reflected in catchment stores.

3.3. Climate modes

(a) Multivariate ENSO Index (MEI)

El-Niño Southern Oscillation (ENSO) is a climate pattern that describes the presence of abnormally warm (El-Niño) and cold (La-Niña) sea surface temperature anomalies in the eastern Pacific (e.g., Phillips et al., 2012). Although there are other ENSO indices such as Nino3.4 and Nino4, the Multivariate Enso Index (MEI) downloaded from NOAA (http://www.esrl.noaa.gov /psd/enso/mei/) is used here because it has been associated with inter-annual variability of water availability, and comprises six other variables over the Pacific coupled with atmospheric anomalies (see, e.g., Phillips et al., 2012; Hurkmans et al., 2009).

(b) Indian Ocean Dipole (IOD)

The Indian Ocean Dipole (IOD) is a coupled ocean and atmosphere phenomenon in the equatorial Indian Ocean that mostly affects the climate of countries around the Indian Ocean (e.g., Saji et al., 1999). It is essentially mirrored in the the SST data over the Indian ocean (Cai et al., 2014). Indian Ocean SSTs have been associated with regional climate anomalies (Bader and Latif, 2003). Apart from ENSO, IOD is one of the relevant climate indices that has been identified as having a robust relationship with Sahel inter-annual rainfall variability (e.g., Okonkwo, 2014). The IOD time series can be accessed from European Climate Assessment & Data portal (http://climexp.knmi.nl)

(c) Atlantic Multi-decadal Oscillation (AMO)

The AMO is a consistent pattern of variability in the North Atlantic SSTs with a period of about 60-80 years, and conventionally computed from the average SST anomaly of the North

Atlantic, that is, north of the equator (see, Trenberth and Shea, 2006). Zhang and Delworth (2006) and Trenberth and Shea (2006) have linked multi-decadal variations of Sahel summer rainfall to AMO. More recently, Chylek et al. (2016) showed that AMO contributed to the $1970-2005$ global warming. In addition, its relative influence according to the study, is expected to increase during the second half of the twenty-first century, further necessitating the need to examine its possible contribution to TWS. The AMO index used in this study was smoothed from the Kaplan SST V2, which is available for downloaded at NOAA's website (http://www.esrl.noaa.gov/psd/data/timeseries/AMO/). The time series of all climate indices used in the study are indicated in Fig. 2.

4. Methodology

4.1. Independent Component Analysis (ICA)

The ICA is a higher order statistical method that uses statistical moments higher than second order. The method uses a statistically based identification technique to estimate directional vectors (i.e., independent patterns) from a data matrix (see, e.g., Common, 1994; Cardoso and Souloumiac, 1993; Cardoso, 1999). The method explores the unknown dynamics of a system through the rotation of the classical empirical orthogonal functions (Aires et al., 2002). Fundamentally, ICA decomposes the time series of the data matrix $\mathbf{Z}_P(t)$, into a mixing matrix A and a number of statistically independent source signals $s_j(t)$, where t is the time index. This can be expressed as (e.g., Ziehe, 2005)

$$\mathbf{Z}_P(t) = \sum A_{ij} s_j(t), \qquad (i = 1, ..., n, \quad j = 1, ..., m). \tag{2}$$

Further details on the computational routines, numerical steps of ICA implementation, algorithm development, and mathematical formulations have been documented (e.g., in Cardoso, 1991; Cardoso and Souloumiac, 1993; Common, 1994; Cardoso, 1999; Theis et al., 2005; Ziehe, 2005). The interest in regionalizing hydro-climatic signals at global and basin scale is increasing and has resulted in several applications of ICA in geophysical signal separation and drought analysis (see, e.g., Ndehedehe et al., 2016b, 2017; Boergens et al., 2014; Forootan et al., 2012, 2014; Frappart et al., 2010, 2011). Here, the ICA (algorithm available at http://perso.telecom-paristech.fr/cardoso/Algo/Jade/jadeR.m) is employed to decompose GRACE-derived TWS (after removing the annual and semi-annual parts) and gridded SPI values into statistically independent modes (spatial and temporal patterns). Note that MERRA-TWS was not statistically decomposed as it does not contain groundwater component, however, since it is sensitive to climate, our focus is to examine and highlight the association of long term TWS changes

with climate teleconnection indices. The temporal evolutions of residual TWS (Section 4.2) were correlated with time series of ENSO, IOD, and AMO in order to assess their association with the observed TWS, which have been localized over West Africa using the ICA technique. ICA is employed to help the regionalization (i.e., localization) of GRACE-TWS values with the hope of studying their association with global climate teleconnections at large spatial scales. The advantage of using ICA for this region, is that it improves the detection of regionally less dominant (i.e., obscured) signals (i.e., those of GRACE-derived TWS) and enables their spatial patterns to be localised making it possible for them to be examined concurrently with the association of climate modes, TWS and SPI evolutions in different sub-regions. Furthermore, since rainfall in West Africa results in two homogeneous regions depending on the domain size and period investigated (e.g., Sanogo et al., 2015), the ICA technique was also employed to support the localisation of complex SPI signals and definition of regions with similar hydro-meteorological patterns in West Africa. It was pointed out in a recent study that regions in West Africa (especially the coastal areas) with large amplitudes of TWS are mostly areas that receive considerable rainfall, characterised by huge aquifers and endowed with surface waters such as lakes and reservoirs (see, Ndehedehe et al., 2016a). Because TWS variability over West Africa is largely precipitation driven, climate teleconnection induced changes in precipitation such as the 2007 and 2010 La-Niñas may have caused larger changes in TWS in the region. In this study, our aim is to understand these modes of extreme precipitation anomalies in the region as they can provide a clue regarding the mechanisms of larger changes in TWS. To this end, the ICA method was also applied to regionalize (localize) SPI patterns (hereafter called drought and wet conditions) over West Africa, in order to help examine the impacts of regional fluctuations in rainfall on catchment storage.

4.2. Multiple Linear Regression Analysis (MLRA)

The strongest signals in TWS variability emanates from the harmonic components (i.e., annual and semi-annual signals) of the data, hence the trend, annual, and semi annual components of the data were removed in order to allow for the estimation of the impact of climate indices. Essentially, our approach employs a MLRA model that parameterizes the cosines and sines' harmonic components of monthly GRACE and MERRA data. This is followed by the method of least squares, which is used to estimate the amplitude of a climate index (i.e., ENSO, IOD, and AMO) on the TWS whose trend and harmonic components have been removed (hereafter called deseasonalize TWS) over the region. Using the MLRA, the dataset

$\mathbf{Y}_{TWS}$, is parameterized as

$$\mathbf{Y}(l,k,t) = \beta_0 + \beta_1 t + \beta_2 sin(2\pi t) + \beta_3 cos(2\pi t) + \beta_4 sin(4\pi t) + \beta_5 cos(4\pi t) + \beta_6 E(t+\varphi_E) + \varepsilon(t), \tag{3}$$

where (l,k) are the grid locations, t is the time in years, β_0 is the constant offset, β_1 is the linear trend, β_2 and β_3 account for the annual signal while β_4 and β_5 represent the semi-annual signal. The variable β_6 is the amplitude of TWS changes or rainfall that is related to climate indices describing large scale ocean-atmosphere phenomenon (e.g., ENSO, IOD, and AMO). E is the normalized time series (i.e., after removing long term mean) of each climate index (Fig. 2), φ_E is the phase lag between the time series of TWS and each climate index, while $\varepsilon(t)$ is the random error term. The annual and semi annual amplitudes of TWS (MERRA and GRACE) over the region are computed as

$$Annual\ Amplitude = \sqrt{(\beta_2)^2 + (\beta_3)^2}, \tag{4}$$

and

$$Semi\ Annual\ Amplitude = \sqrt{(\beta_4)^2 + (\beta_5)^2}. \tag{5}$$

Removing these harmonic components and the trend in Eqn 3 leaves the residual part, (i.e., deseasonalized TWS, $\mathbf{X}_{TWS}$) which is here assumed to be associated with slow dynamic climate oscillations (e.g., AMO). This residual variability perhaps can also emanate from internal variability or regional forcings (though unclear for the region), but as indicated in Section 1, the impact of climate related indices on rainfall are more likely to result in large amplitudes of TWS, dominating the time series of the deseasonalized TWS. This deseasonalized TWS is statistically decomposed into temporal and spatial patterns (i.e., using the ICA technique described in Section 4.1). The deseasonalized $\mathbf{X}_{TWS}$, signal is characterised as

$$\mathbf{X}_{TWS} = \mathbf{Y} - [\beta_1 t + \beta_2 sin(2\pi t) + \beta_3 cos(2\pi t) + \beta_4 sin(4\pi t) + \beta_5 cos(4\pi t)]. \tag{6}$$

The coefficients of MLRA indicated in Eqns 4-6 were estimated using the least square adjustment technique. The linear trend of TWS is removed in order to ensure that the pseudo trends (GRACE-TWS) emanating from the ponding of water behind large dams as is the case in Lake Volta (e.g., Ndehedehe et al., 2017; Moore and Williams, 2014) are not interpreted as contributions of climate modes to TWS changes. This deseasonalized TWS was statistically decomposed into spatial and temporal patterns using the ICA technique (see Section 4.1). The significant modes of variability of the deseasonalized TWS were selected for a further comparison with the normalised time series of each climate index. Doing this allows the evaluation of the quantitative estimates of climate induced TWS in terms of the variability explained.

Further, in order to estimate the contribution of each of the climate index (i.e., ENSO, IOD, and AMO) on the amplitudes of GRACE and MERRA-derived TWS, a least square fit on each grid location of $\mathbf{X}_{TWS}$ in Eqn 6 was then performed as (e.g., Phillips et al., 2012)

$$\mathbf{X}_{Indices}(x,y) = a(x,y) + b(x,y) * Indices + c(x,y) * imag(Hilbert(Indices)), \tag{7}$$

where coefficients b and c are used to estimate the climate induced TWS change $\mathbf{X}_{Indices}(x,y)$ at a grid location (x,y), while the imaginary part of the Hilbert transform of the climate index represents the lag between TWS anomalies and a given climate index (see, Phillips et al., 2012). The amplitude of TWS, A, given as

$$A_{ENSO/IOD/AMO} = \sqrt{b^2 + c^2}, \tag{8}$$

is the estimated magnitude of climate index on TWS (i.e., the estimated contribution of each of the climate index to TWS change).

4.3. Standardised Precipitation Index (SPI)

Prolonged rainfall deficit usually reduces the alimentation of a given hydrological system leading to agricultural and hydrological drought (see, Ndehedehe et al., 2016c). It is reasonable therefore to assume that extreme rainfall conditions (i.e., wet and drought events) resulting from the influence of climate teleconnections on the region will have a direct impact on the amplitudes of TWS perhaps with some time lags of say 6-12 months. To this end, extreme rainfall conditions are analysed using SPI aggregated at 6 and 12 months. The choice of these aggregation scales is based on the hypothesis that SPI on longer time scales can provide the capability to monitor drought and wet conditions suitable for hydrological applications (see, e.g., Ndehedehe et al., 2016c; Li and Rodell, 2015; Lloyd-Hughes, 2012; Hayes et al., 1999), which is what MERRA and GRACE-derived TWS are mostly suited for (e.g., Awange et al., 2016). For example, Li and Rodell (2015) recently showed that averaged groundwater drought index had a strong correlation with SPI at 12 and 24 month cumulations. To understand the influence of climate induced rainfall conditions on observed TWS over West Africa, SPI (McKee et al., 1993) was computed from the GPCP based precipitation for the period $1979 - 2014$. Instead of the gamma distribution, log-normal, extreme value, and exponential distributions that have been widely used in the simulations of precipitation distributions (e.g., Mishra and Singh, 2010), this study uses a non-parametric approach to derive standardised index (see, Farahmand and AghaKouchak, 2015; Hao and AghaKouchak, 2014). Although the gamma distribution, for instance, is efficient for low runoff values as noted by Shukla and Wood (2008), the sensitivity of the traditional SPI tails to distribution parameters (e.g., Farahmand

Table 2: SPI thresholds based on McKee et al. (1993) classification system.

Description	Threshold
Extreme wet	+2.0 and above
Very wet	+1.5 to +1.99
Moderately wet	+1.0 to +1.49
Near normal	-0.99 to +0.99
Moderate drought	-1.0 to -1.49
Severe drought	-1.5 to -1.99
Extreme drought	-2.0 or less

and AghaKouchak, 2015), however, may lead to inconsistent results for different regions. The non-parametric approach on the other hand can be applied to different hydro-climatic data (e.g., precipitation) without having to assume representative parametric distributions (see, Farahmand and AghaKouchak, 2015). This approach employs an empirical probability method as

$$\rho(x_j) = \frac{j - 0.44}{n + 0.12}, \tag{9}$$

where n is the sample size, j represents the rank of non-zero rainfall data starting from the smallest while $p(x_j)$ is the corresponding empirical probability. Equation 9 is transformed to a standardised precipitation index (SPI) as (see, Farahmand and AghaKouchak, 2015)

$$SPI = \phi^{-1}(\rho), \tag{10}$$

where ϕ is the standard normal distribution function and ρ is the probability obtained from Eqn 9. The SPI values obtained from Eqn 10 were subsequently decomposed into spatial and temporal patterns using the ICA technique (see Section 4.1). The association of a climate index with the temporal SPI evolutions were examined through Pearson's correlation analysis. Dry and wet occurrence in this study is based on the McKee et al. (1993) classification system as highlighted in Table 2.

5. Results and Discussion

5.1. Extreme hydro-meteorological conditions related to climate modes

This section relates extreme hydro-meteorological conditions (drought and wet conditions based on the description of Table 2) to climate modes using a spatio-temporal approach where the SPI values obtained over West Africa are statistically decomposed into spatial and temporal patterns. For the 6 month SPI localised over the region, the spatio-temporal patterns show

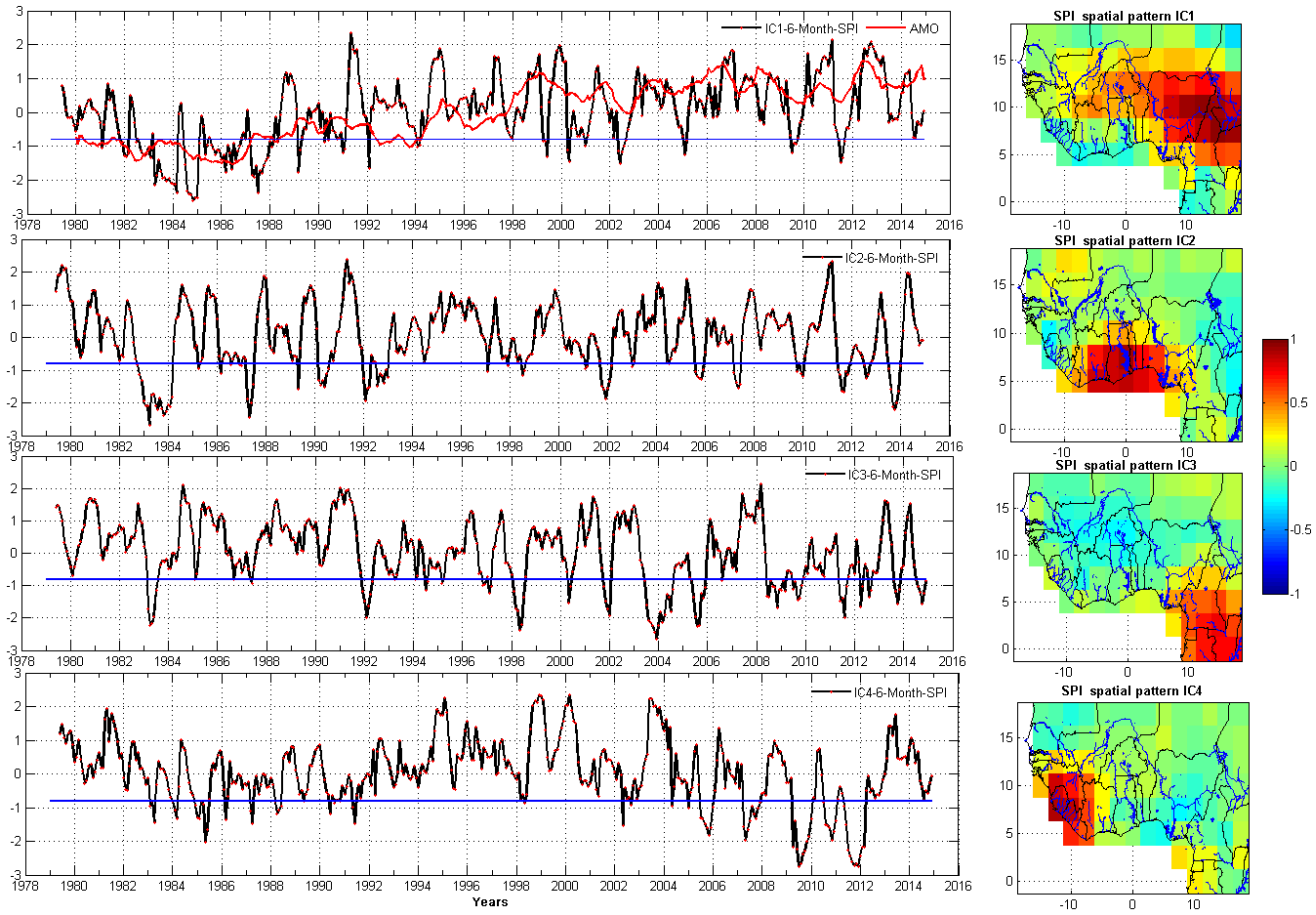

Figure 3: Spatio-temporal SPI patterns over West Africa using 6-month gridded SPI values. SPI values are computed using GPCP-based precipitation product over the period $1979-2014$. The variability of the statistically decomposed SPI values are 14.1%, 7.7%, 7.2%, and 4.6% for IC1, IC2, IC3, and IC4, respectively. Actual values for drought classification and categorization with respect to McKee et al. (1993) description are jointly derived from the localised spatial patterns (right) and their corresponding temporal evolutions (left). The AMO showed relatively a better association with SPI over the Sahel region (IC1) compared to other climate indices (ENSO and IOD). The blue solid line (left) is the drought threshold. Hydrological units (rivers, lakes and other water bodies) are also indicated on the spatial patterns of SPI (blues lines on the right).

the spread of SPI patterns, its frequency, onset, and termination. The observed temporal SPI evolutions (i.e., IC1−IC4, Fig. 3) are consistent with previous drought records of the region (e.g., Masih et al., 2014). The wider spread of droughts in some parts of the Sahel as indicated in the SPI spatial and temporal patterns (IC1, Fig. 3) confirms that the Sahel region was the worst hit by the droughts of $1982-1984$, which affected West Africa and the continent at large. The AMO showed stronger association with SPI in some parts of the Sahel region and Central Africa Republic compared to ENSO and IOD (see IC1, Fig. 3 and Table 3). Although this specific case study indicates that AMO is more associated with the temporal patterns of SPI in much of the Sahel region, extreme wet conditions related to ENSO have also been reported in the region (e.g., Paeth et al., 2012; Nicholson et al., 2000). As shown in the SPI temporal

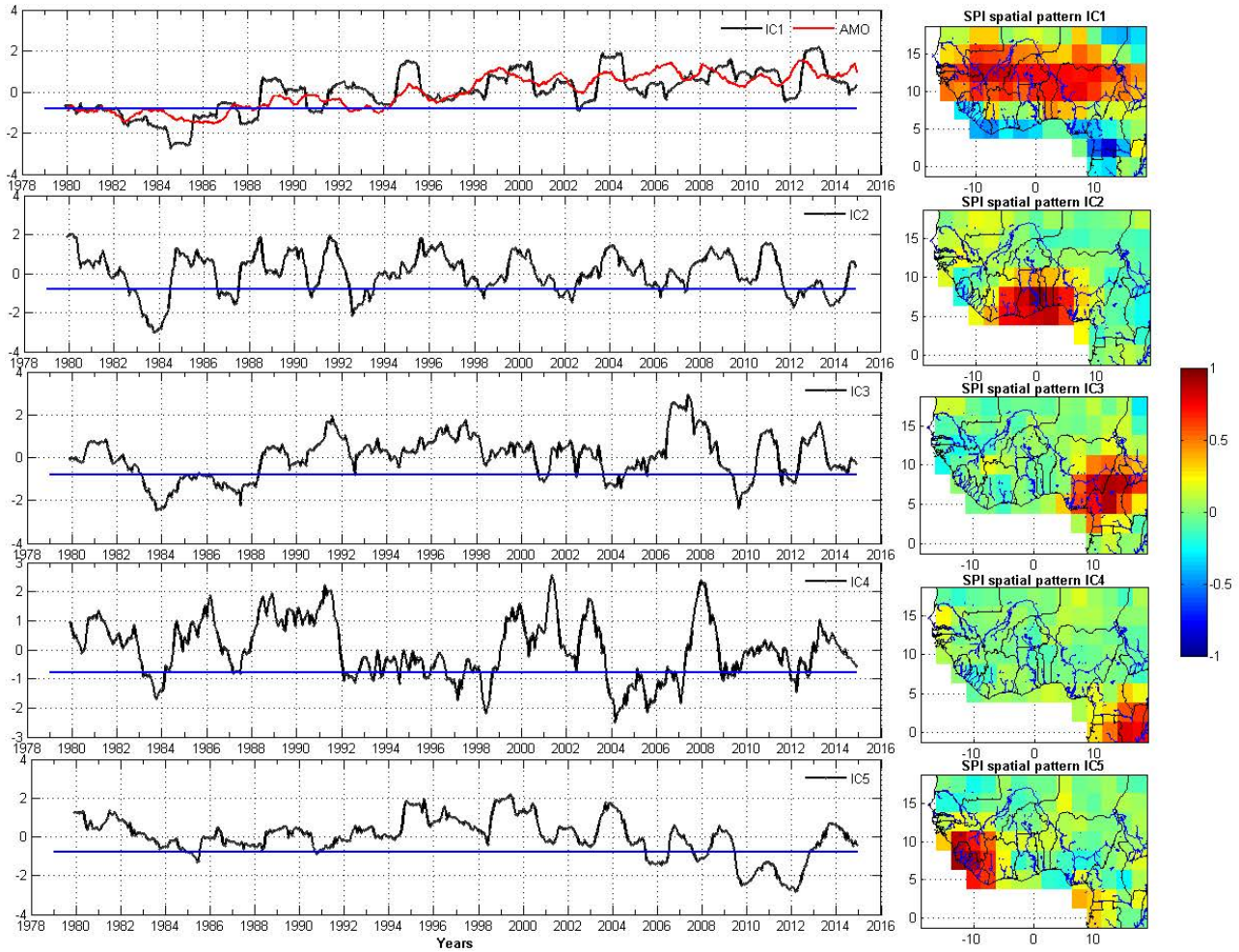

Figure 4: Spatio-temporal SPI patterns over West Africa using 12-month gridded SPI values. SPI values are computed using GPCP-based precipitation product for the period 1979−2014. The variability of the statistically decomposed SPI values are 17.4%, 7.0%, 6.5%, 5.3%, and 5.1% for IC1, IC2, IC3, IC4, and IC5, respectively. Actual values for drought classification and categorization with respect to McKee et al. (1993) description are jointly derived from the localised spatial patterns (right) and their corresponding temporal evolutions (left). The AMO showed stronger association with SPI over the Sahel region (IC1) compared to ENSO and IOD. The blue solid line (left) is drought threshold. Hydrological units (rivers, lakes and other water bodies) are also indicated on the spatial patterns of SPI (blues lines on the right).

patterns (IC1, Fig. 3), 1991, 1998/1999, 2007, and 2010 are instances of wet conditions that could be attributed to ENSO events since they coincide with the ENSO years. Over the Volta basin, 2010 was extremely wet (IC2, Fig. 3) consistent with the strong amplitudes of TWS in the basin (see Section 5.2.1 for more discussion). Although the observed trends in GRACE-derived TWS in the Volta basin have been attributed to the influence of Lake Volta due to water ponding behind the dam (e.g., Ndehedehe et al., 2017; Ahmed et al., 2014), the wet conditions of the late 2007/2008, and 2010 associated with ENSO event (IC2, Fig. 3), resulted in water level rise of up to 7 m in 2010 over the lake (see, Ndehedehe et al., 2016a, 2017). Strong fluctuations in SPI temporal patterns that coincided with ENSO events have also been

highlighted in the Congo basin and some countries of the Guinea Coast (Liberia, Guinea, and Sierra Leone) (IC3-IC4, Fig. 3).

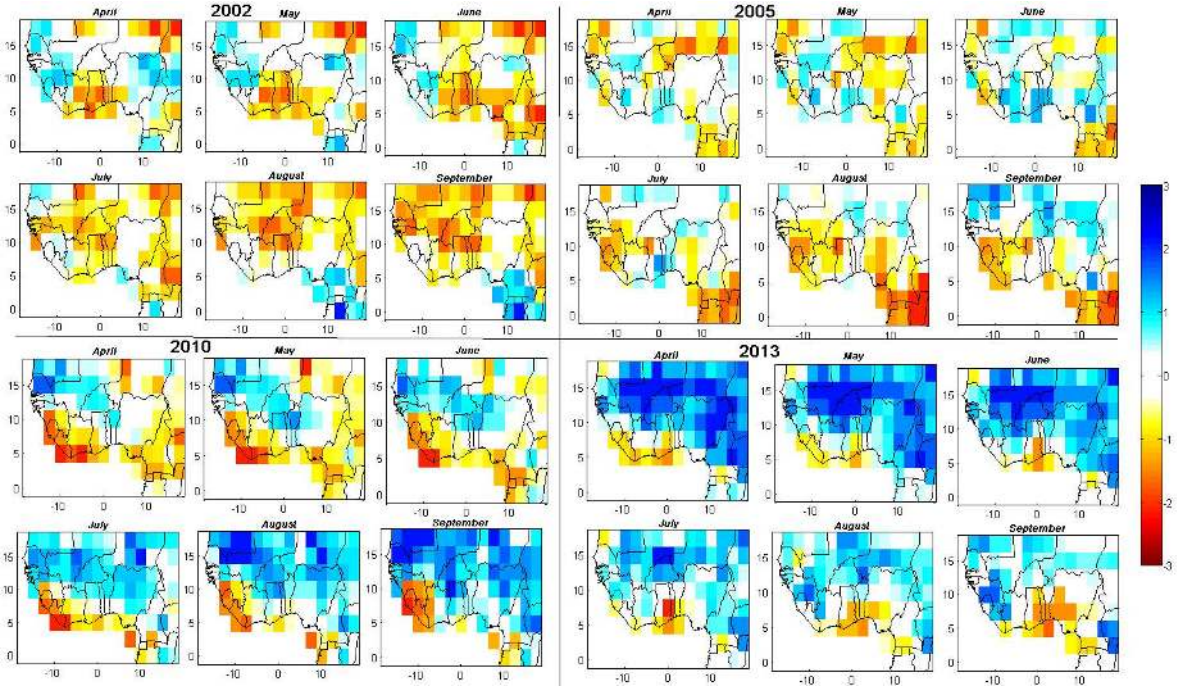

Figure 5: Space-time evolution of SPI (i.e., 12 month aggregation) patterns for 2002, 2005, 2010, and 2013 over West Africa. Unlike Figs. 3 and 4 these SPI patterns have not been localised.

At the 12 month SPI, the Sahel seems to be extremely wet in 1994/1995, 1998/1999, 2003/2004, and recently during the $2012-2014$ period (IC1, Fig. 4). Nicholson et al. (2000) reported similar wet conditions for 1988 and 1994 emphasizing a long term change in rainfall over the region. Depending on the structural stability, hydraulic conductivity, infiltration, and soil water holding capacity of the Sahel (see, Descroix et al., 2009), extreme wet conditions such as the 2003/2004 and the $2012-2013$ period (IC1, Fig. 4) may translate to huge catchment storage and inundated areas, leading to increase in TWS (Ndehedehe et al., 2016a). Apart from a wider SPI spatial distribution along the Sahel band, it is noticeable that the extreme droughts of the 1980's in the Sahel region (IC1, Fig. 4) persisted a bit longer ($1982-1985$) at the 12 month aggregation when compared to 6 month SPI (IC1, Fig. 3). Further, the Volta basin show wet conditions, for example, in 2010 (IC2, Fig. 4) similar to what is observed in the 6 month SPI aggregation (IC2, Fig. 3). The wet conditions of 2007 in Cameroon/Nigeria and Congo maybe ENSO-related (IC3 and IC4, Fig. 4), due to the fact that multiple strings of El-Niño and La Niña episodes have been reported, for example, in Cameroon and the Congo basin (e.g., Molua and Lambi, 2006).

Lake Volta, a major physiographic feature seated in the southern part of the Volta basin derives its nourishment from the Volta river system (comprising the Black Volta, White Volta,

Table 3: Correlations between ICA-decomposed SPI-6/SPI-12 month temporal drought evolutions and climate indices. The correlation coefficient in bold are statistically significant at the 95% confidence level using the Student T-test.

ICs/Region	**AMO**	**IOD**	**ENSO**
IC1 (Sahel)	**0.43/0.62**	0.12/0.12	**-0.22/-0.22**
IC2 (Volta basin)	-0.01/-0.01	0.02/0.01	**-0.30/-0.30**
IC3 (Congo basin/Nigeria)	**-0.33/0.30**	-0.09/0.11	**-0.21**/-0.14
IC4 (Guinea Coast/Congo)	**0.30/-0.17**	0.15/0.0	**0.18/-0.30**
IC5 (Guinea Coast)	-0.01/-0.09	-0.01/-0.06	-0.03/0.03

and Oti Rivers). Besides the rainfall in Ghana and the Oti river that also contribute to the TWS around the Lake area, the Black and White Volta rivers have their sources in Burkina Faso and contribute about 30% of the total annual flow to Lake Volta (e.g., Barry et al., 2005). This implies that the magnitude of wet conditions in Burkina Faso, for example, during $2012-2013$ (IC1, Fig. 4) and Ghana for the $2008-2009$ and $2010-2011$ periods (IC2, Fig. 4) may induce considerable changes in regional hydro-meteorological patterns leading to large amplitudes of TWS in the basin. Similarly, as the reservoir system of the Lake Volta is naturally connected to the Volta river system (see, Ndehedehe et al., 2017), climate teleconnection-induced reductions in rainfall may directly impact on the stream flows of the Volta river system, leading to deficits in stored water of the basin. Furthermore, the SPI spatial evolutions (i.e., without statistical decomposition) were sampled for the April-September months when considerable and significant rainfall occur in the region. This was done specifically for 2002, 2005, 2010, and 2013. The SPI spatial distribution for the year 2002 (Fig. 5) confirms the severe wet and dry conditions previously observed in Ghana and countries in the Sahel (IC1-IC3, Fig. 4). The Sahel also show wet conditions in 2010 and 2013 (Fig. 5) while Liberia and Sierra Leone indicate extreme drought condition (though 2013 was moderate drought) during the same period consistent with IC1 and IC5 of Fig. 4, respectively. Overall, the SPI spatial patterns (Fig. 5) are consistent with the ICA-derived spatial evolutions of wet and dry conditions (Figs. 3 and 4).

The association of SPI temporal evolutions (i.e., all the independent components of Figs. 3 and 4) with climate teleconnections were also evaluated. The temporal evolutions of SPI cumulated at 6 and 12 months (Figs. 3 and 4) were correlated with ENSO, AMO, and IOD. The results show that AMO is associated with extreme dry and wet conditions in the Sahel (i.e., IC1, Figs. 3 and 4), indicating statistically significant (at 95% confidence level) positive

correlations of 0.43 and 0.62 with time series of SPI 6 and 12 months aggregations, respectively. The correlation results of these climate teleconnections with temporal evolutions of SPI over West Africa, which have been summarised in Table 3 also show negative correlations of -0.30/0.30 (ENSO), -0.33 (AMO) and positive correlation of 0.30 (AMO) with SPI temporal evolutions in the Volta and Congo basin areas (i.e., IC2 and IC3 of Fig. 3 and IC2 and IC4 of Fig. 4).

While ENSO and AMO explain some of the variability in the observed rainfall conditions in West Africa, IOD does not show a statistically significant relationship as most correlations are relatively weak and statistically insignificant. However, as mentioned earlier, the droughts of the 1980's in the Sahel were attributed to the synergy between the abnormally warm Indian Ocean SST and that of the eastern Atlantic, which suppressed rainfall in the Sahel due to large scale subsidence in the troposphere (see, Bader and Latif, 2011). Given that IOD is a coupled ocean and atmosphere phenomenon mirrored in the the SST data over the Indian Ocean (see, Cai et al., 2014; Saji et al., 1999), the impact of SST from the Indian Ocean, which is reported to have induced dryer conditions in the Sahel, are usually facilitated and induced by an occasionally warmer-than-average SST of the Atlantic Ocean (Giannini et al., 2003). Our hypothesis is that such impact, coupled with the association of ENSO and AMO on rainfall fluctuations as observed over the region, could be related to changes in TWS over West Africa. In Sections 5.2.1 and 5.2.2, such possibilities are further investigated using a combination of MLRA, Pearson correlation and statistical decomposition method (i.e., the ICA).

5.2. Terrestrial water storage variability and its association with climate teleconnections

5.2.1. Relationship between climate modes and deseasonalized TWS changes

As a result of diversity in local climate in West Africa, which is mostly regulated by the movement of the rainbelt and other meteorological processes, similar to rainfall, TWS appears to be dominated by annual and semi annual patterns. For example, considerable strong annual and semi annual amplitudes of GRACE and MERRA-TWS are mostly found in Guinea and much of the Congo basin (i.e., in Gabon and Congo), respectively (Figs. 6a-d) where rainfall is mostly annual and bimodal. Also, relatively strong TWS amplitudes of about 300 mm and more at the annual scale are found in Nigeria, Cameroon, and Central African Republic (Fig. 6a), all of which are located in the humid parts of the study area. These humid parts of West Africa are mostly characterised by networks of rivers, lakes, and several groundwater aquifers (Fig. 1). Essentially, as highlighted in a previous report (Ndehedehe et al., 2016a), these TWS amplitudes are induced by a relatively strong annual and seasonal

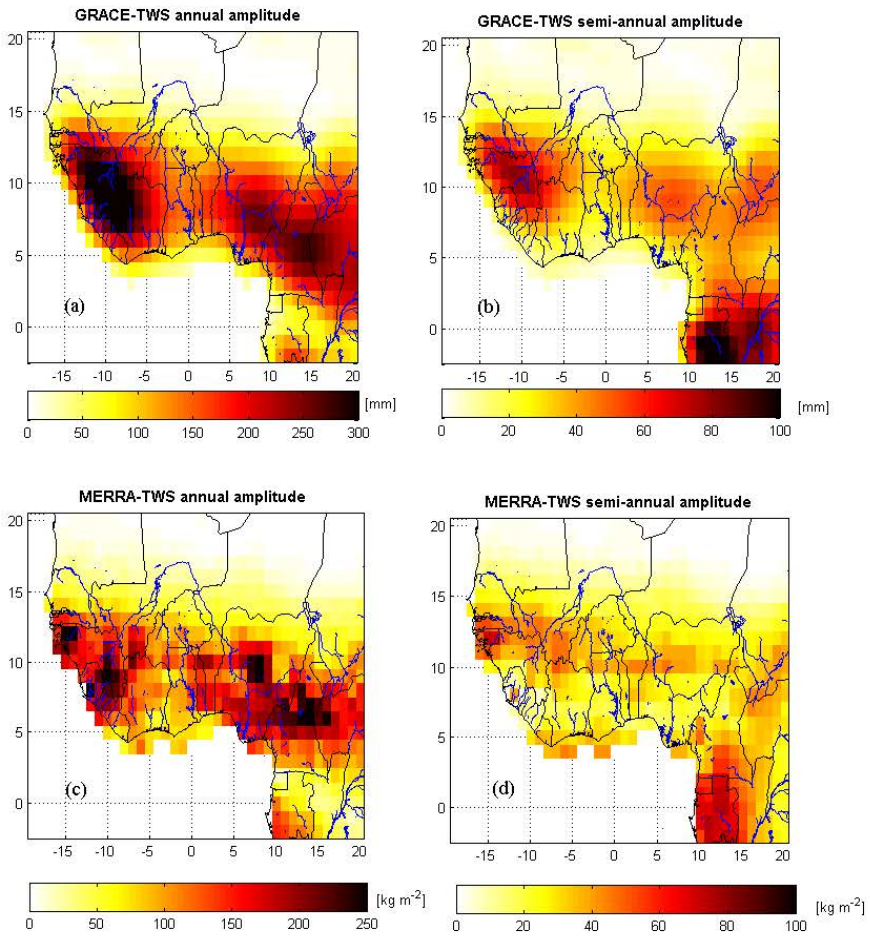

Figure 6: Spatial patterns of annual and semi annual amplitudes of GRACE-derived TWS ($2002 - 2014$) and MERRA-TWS ($1980 - 2015$) over West Africa using the MLRA.

rainfall patterns, in addition to the presence of surface waters as is the case in the Congo basin and Nigeria. Moreover, the annual and semi annual amplitudes of GRACE-TWS (Figs. 6a and b) are stronger than those of MERRA-TWS (Figs. 6c and d) probably due to the lack of groundwater and surface water component in the MERRA reanalysis data. Reanalysis data such as the MERRA-TWS may not be excellent representations of the real system, however, they are furnished with numerical weather predictions and observations and are extremely useful in circumstances where observations are lacking and insufficient. It is further observed that the semi annual amplitudes of TWS dominates the equatorial regions (specifically Gabon and Congo) (Figs. 6b and d) while Guinea is the only country with relatively strong annual and semi annual amplitudes of TWS (Figs. 6a-c) in West Africa.

As opposed to the Sahel region, the considerable strong annual and semi annual patterns of TWS in the Guinea Coast countries and Congo basin (Figs. 6a-d) confirm that these areas are the most favourable hydrological environments. Precipitation in these areas are largely seasonal and bimodal, and are driven by numerous factors, such as atmospheric circulation

features, mesoscale convective systems, ocean warming, physiographic features, and other processes of oceanic inter-annual variability (see, e.g., Hua et al., 2016; Mohino et al., 2011; Paeth et al., 2012; Bader and Latif, 2011; Boone et al., 2009; Giannini et al., 2008). In Guinea, for example, where GRACE-TWS annual amplitude is the strongest in the region (Fig. 6a), topography also play key roles in rainfall variability. Generally, high elevation areas in coastal West Africa tend to be characterised by stronger amplitudes of rainfall. While the role of topography on hydrological conditions remains a subject for future considerations, these rainfall patterns provide significant controls on inter-annual and inter-decadal variability in river flows and TWS in the region (see, Ndehedehe et al., 2016a; Conway et al., 2009). Interestingly, the groundwater maps of Africa developed by MacDonald et al. (2012) also show that these coastal areas of West Africa have higher recharge and the shallowest groundwater-levels (i.e., < 7 mgbl) compared to the Central Sahel ($50-250$ mbgl). While these groundwater maps also show that considerable amount of groundwater volumes exists in large sedimentary aquifers in North African countries, the distribution of freshwater and the huge water fluxes in coastal West Africa (e.g., Andam-Akorful et al., 2017; Ndehedehe et al., 2016a), is generally consistent with the amplitudes of TWS indicated in Fig. 6. Major rivers (e.g., the Niger, Congo, and the Volta river systems), which drain the region (cf. Fig. 1), in addition to the numerous dams and reservoirs (e.g., Kainji, Akosombo, Kindia, Konkoure, etc.) serving hydropower purposes are indications of the active hydrological nature of the region. As will be highlighted later in the manuscript (Section 5.2.2), the temporal and spatial distributions of TWS in these areas are also largely driven by teleconnections amongst other factors, similar to rainfall.

The relationship of climate modes with deseasonalized TWS (i.e., the localised TWS signals from the ICA procedure) was examined in the region. As indicated in Fig. 7, the ICA technique localises the TWS changes, providing a more meaningful space-time patterns that can be associated with physical phenomena. Similar to Ilin et al. (2005) who identified the ENSO phenomenon in global climate data (surface temperature, sea level pressure and precipitation) using signal separation techniques, the main target here is to identify physically meaningful oscillations of the climate system that disturbs the region's hydrology and impacts on freshwater distribution and variability. In order to predict TWS changes in West Africa, Forootan et al. (2014) combined the ICA technique with an autoregressive model to statistically study the physical processes of the region (excluding countries of the Congo basin). Whereas they focused on developing a prediction model based on independent temporal series of TWS, sea surface temperature and rainfall, the approach in this study identifies indepen-

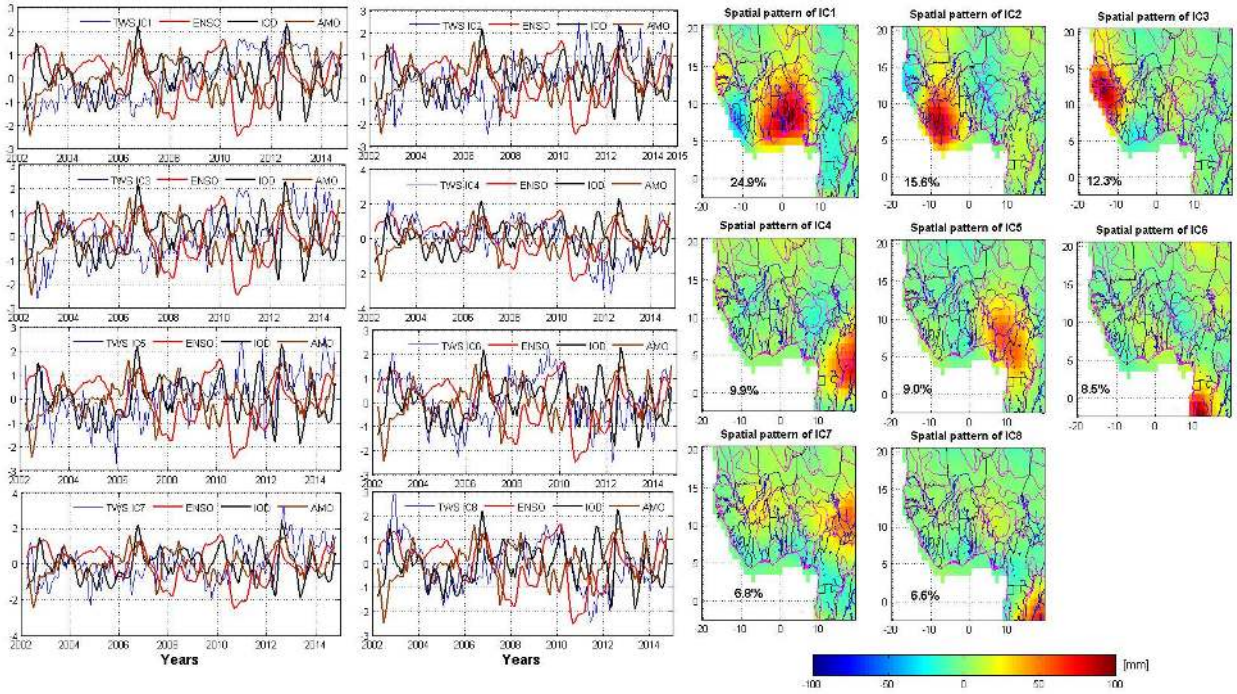

Figure 7: ICA decomposition of GRACE-derived TWS (2002 – 2014) over West Africa after separating the annual and semi annual cycles (i.e., deseasonalized) using the MLRA. The independent components (left) are temporal patterns which are unit-less and corresponds to the spatial patterns (right), which have been scaled using the standard deviation of the computed independent components of GRACE data. The total variabilities explained by each ICA mode are also indicated. Other hydrological units (rivers, lakes, and groundwater aquifers) have been indicated on the spatial patterns (blues and magenta lines on the right) associated with the temporal series of SPI (left)

dent spatial elements of TWS over West Africa (including the Congo basin) with potential connections to climate modes. The ICA modes analysed in this study (Fig. 7), however, show variability in TWS (spatial patterns) over the Guinea Coast countries and some Sahelian areas that compares well with the leading modes of TWS presented by Forootan et al. (2014). In addition to this, spatially independent patterns of TWS are also observed over the Congo basin area (Fig. 7). ENSO shows a statistically significant negative correlation of -0.40 with TWS (IC1, Fig. 7), suggesting that ENSO explains some of the observed variability in TWS over the Volta basin and some parts of Nigeria. A coupled association of ENSO and AMO in Guinea and Chad is also noticed as they both indicate negative correlations of -0.30 with ENSO, while AMO shows weak positive correlations of 0.23 and 0.24, respectively with TWS (Table 4). Also, in Gabon, weak correlations of 0.20 and -0.22 for IOD and AMO, respectively with TWS (IC6, Fig. 7) are found. The correlation results of the climate teleconnections with the temporal evolutions of TWS over West Africa are summarised in Table 4. We do not claim any cause-effect relationship in the correlation results of TWS and climate indices. Considering that some of the strong peaks (wet or dry) observed in the SPI shown in Figs. 3 and 4

(i.e., the SPI orthogonal modes) are climate indices related, the catchments within the Guinea Coast and Equatorial regions then become direct recipients of these extreme conditions. In the course of time (e.g., 1 year or more), probably owing to hydraulic characteristics of the region, the impact of these indices are likely to be reflected in storage conditions. We are cautious about this speculation, but Dong et al. (2015), in addition to observing an ENSO-induced variance in aquifer water levels in Japan, found that the water level in recharge area mainly fluctuates between 1 and 2-year periods. Given that ENSO and AMO were associated with drought temporal evolutions in the region (see Section 5.1), their association with TWS (Fig. 7) might be expected as rainfall is a major driver of TWS in the region (Ndehedehe et al., 2016a). The AMO for instance, shows a correlation of 0.62 with SPI 12 month time series while ENSO indicates a statistically significant negative correlation of -0.30 with time series of SPI 6 month cumulation.

Observing more closely, one notes that unlike in the $2002-2007$ period, Liberia and parts of Guinea/Ivory Coast/Seirra Leone indicated a considerable high pronounced amplitudes of TWS between 2010 and 2013 (IC2, Fig. 7), inconsistent with extreme drought conditions during the same period when drought persisted during the $2009-2012$ period (IC5, Fig. 4). Although meteorological patterns in these countries (Guinea/Ivory Coast/Seirra Leone) are associated with El-Niño events amongst other factors, large inter-annual variability in annual and seasonal rainfall, huge catchment stores, and the cumulative increase in the volume of water not involved in surface runoff (Ndehedehe et al., 2016a) are possible reasons for this inconsistency. There are indications, nonetheless, that these countries, which also indicate the strongest annual amplitude of TWS (Fig. 6a) show the presence of climate-induced TWS (Section 5.2.2).

Besides the observed association of ENSO with TWS in the region, our findings also confirm that the development of AMO can also be considered as a factor that could enhance more rainfall in the Sahel leading to significant contributions on TWS changes in the region. AMO in particular showed the strongest associations with rainfall condition (i.e., 0.43 and 0.62 for SPI at 6 and 12 month aggregations, respectively) in the Sahel region (IC1, Figs. 3 and 4). Some studies (e.g., Ndehedehe et al., 2016b; Okonkwo, 2014; Mohino et al., 2011) have shown that the AMO index explains drought characteristics in the Sahel. Whereas Hodson et al. (2010) argued that the AMO played no role in the observed decline in Sahel rainfall, Rodríguez-Fonseca et al. (2011) however, attributed the decline in Sahel rainfall to the combined effects of AMO and global warming SST modes. They also speculated that a change in the AMO phase towards the end of the 20th century could have triggered the partial recovery in Sahel

Table 4: Correlations between ICA-derived temporal evolutions of TWS and climate teleconnections. The correlation coefficient in bold are significant at the 95% significant level using the Student's t-test. The locations of the observed spatial patterns are also indicated.

ICs	ENSO	IOD	AMO	Region
IC1	**-0.40**	0.10	0.12	Volta basin/Nigeria
IC2	**-0.30**	0.08	**0.20**	Liberia/Ivory Coast/Guinea
IC3	**-0.30**	-0.02	**0.23**	Guinea/Senegal/Gambia
IC4	**0.23**	-0.01	0.01	Congo/Central African Republic
IC5	-0.14	0.14	0.19	Nigeria/Cameroon
IC6	0.16	**0.20**	**-0.22**	Gabon
IC7	**-0.30**	0.01	**0.24**	Chad
IC8	**0.30**	0.16	-0.14	Congo/Democratic Republic of Congo

rainfall, consistent with Mohino et al. (2011) who had similar conclusions that the partial recovery was mainly driven by the AMO. The association of AMO with temporal evolutions of SPI over the Sahel region in this study is consistent with Diatta and Fink (2014) who found a positive correlation between Sahel rainfall and AMO. Rainfall over the Sahel is enhanced by the positive phase of the AMO while in the Gulf of Guinea AMO decreases it (Mohino et al., 2011). Consequently, this observed relationship between AMO and localised SPI time series (IC1, Figs. 3 and 4) may have implications on TWS variations (especially the soil moisture components) and ecosystem performance, probably in complex and non-linear ways that would perhaps require further analysis in the future.

5.2.2. Spatial variability of climate induced TWS

The spatial patterns of climate induced TWS presented in Fig. 8 are for areas where statistically significant ($\alpha = 0.05$) relationships (TWS vs teleconnections) exist in the region. The amplitudes of the relative contributions (i.e., from the spatial patterns) of these climate teleconnections on TWS changes were estimated using Eq.8. The amplitudes of GRACE-TWS induced by all three climate modes in the equatorial regions (Gabon, Congo, and Democratic Republic of Congo-DRC) reached 30 mm for ENSO, AMO, and IOD respectively, (Fig. 8a-c). For the long term MERRA-derived TWS, the spatial patterns for all climate-induced TWS indicate an amount greater than 30 kg m^{-2} in the Gulf of Guinea countries and equatorial regions (Fig. 8d-f). The contributions of ENSO, AMO, and IOD are somewhat weak in much of the Sahel but strong along the coastal West African countries probably due to rainfall

distribution patterns, which are modulated by ITCZ and transitions in the rain belt.

Overall, considerable strong contributions of climate teleconnections to TWS change in the region are found mostly in areas with a strong presence of surface water (rivers and lakes), sub-surface storage changes (e.g., groundwater aquifers) and annual rainfall (cf. Figs. 1 and 8d-f). For instance, high rainfall amounts at seasonal and annual scales are prominent drivers of TWS changes over West Africa as highlighted in e.g., Ndehedehe et al. (2016a). But the river discharge of the lower Congo basin, Lake Volta water level variations, and the Chari-Logone river system, which provide approximately 95% of the total input into Lake Chad basin, are also major triggers of observed trends and inter-annual variability in TWS. The

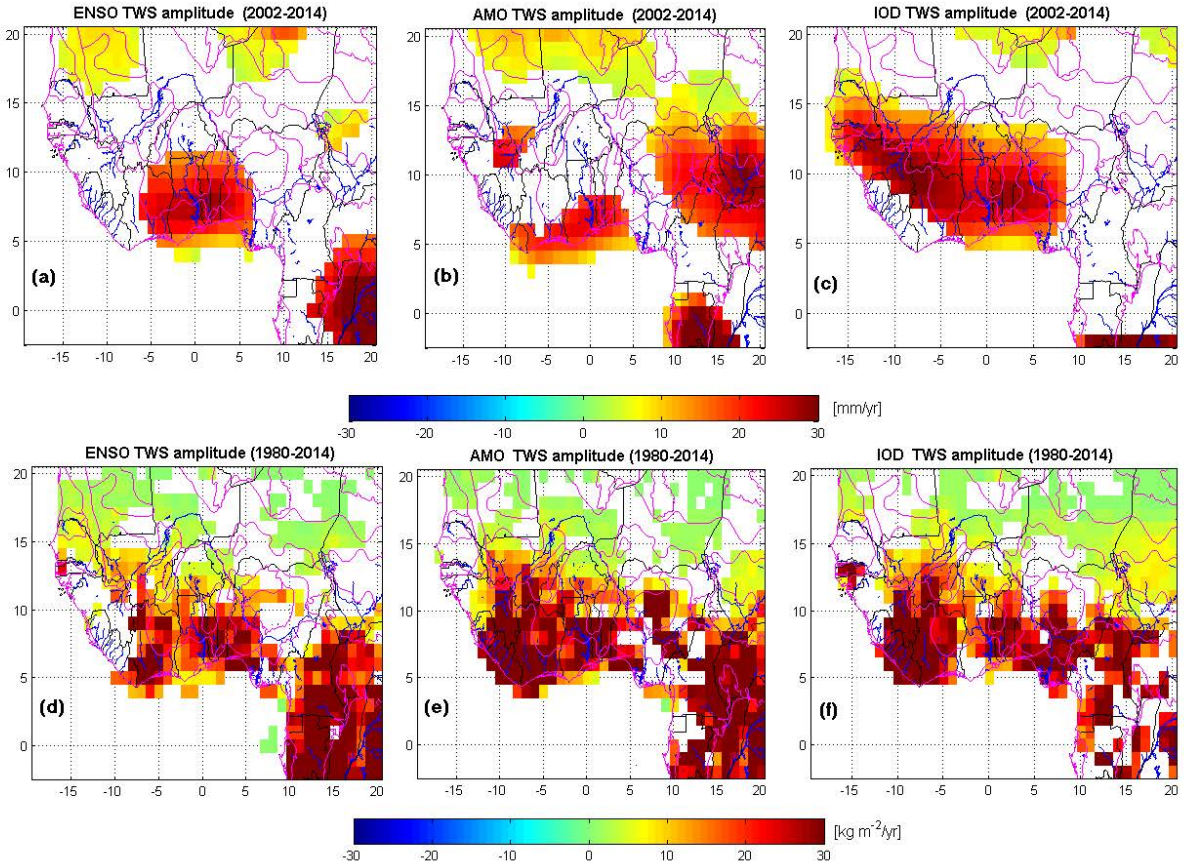

Figure 8: Spatial patterns of climate induced TWS derived from GRACE-TWS (a-c) and MERRA-TWS (d-f). These estimates (amplitudes of TWS) are derived using the MLRA technique. The regression coefficients indicated for both GRACE and MERRA data are those with statistically significant ($\alpha = 0.05$) association with climate indices (ENSO, AMO, and IOD). Groundwater aquifers (magenta), rivers and lakes (blue) have also been shown on the spatial distribution of climate induced TWS.

ENSO-induced amplitude of TWS indicated by GRACE and MERRA are relatively strong and have a wider spread over the Volta and Congo basins (Figs. 8a and d) compared to the Sahel while the amplitude of AMO-induced TWS show strong presence in much of the Guinea Coast areas and the equatorial regions where rainfall is relatively high and bimodal

(Figs. 8b and e). Recall that in Section 5.2.1, the temporal evolutions of TWS over the Volta basin (IC1, Fig. 7) showed a statistically significant negative correlation of -0.40 with the normalised time series of ENSO. This observed relationship is moderate and also coincides with the negative correlation of ENSO (i.e., -0.30) with the temporal evolutions of SPI 6 and 12 months aggregation (see Table 3), indicating that ENSO has an association with rainfall conditions and TWS changes over the Volta basin. The ENSO phenomenon has been linked to increase in the variability and decline in rainfall totals, causing decline in Lake Volta water levels (Owusu et al., 2008). Other regions such as the Congo basin also indicate similar association with ENSO, that is, positive correlations of 0.23 and 0.30 with TWS (IC4 and IC8, Fig. 7, respectively) and a negative correlation of -0.30 with SPI temporal evolutions (IC7, Fig. 7). Besides the associations of ENSO and AMO with rainfall conditions, we also found a somewhat weak correlation of IOD (0.20, Table 4) with temporal patterns of TWS in Gabon (IC6, Fig. 7, respectively). In addition to the observed relationship of IOD with the temporal patterns of TWS in Gabon, the contributions of IOD-induced TWS (GRACE), which reached 30 mm (Fig. 8c) may suggest a possible contribution of all three climate modes in this sub-region. Coincidentally, the spatial patterns of IOD-induced TWS (GRACE) are in the same direction where increasing trend in GRACE-TWS was observed in previous studies (Ndehedehe et al., 2016a; Ahmed et al., 2014). However, the magnitude and domain size of MERRA-TWS indicates that ENSO and AMO have had stronger impact on the TWS of the region during the $1980-2015$ period (Fig. 8d and e) compared to IOD (Fig. 8f).

The impact of the frequency and strength of IOD on the West Africa's climate is still unclear. Bader and Latif (2011) and Giannini et al. (2003) have argued however, that the warming in the Indian Ocean was a major forcing in the observed 1983 drought in the West Sahel. Whereas IOD indicates contributions of more than 30 kg m^{-2}/yr in the long term MERRA-TWS in east Guinea (part of West Sahel), Côte d'Ivoire, Benin, Nigeria, Liberia, and the equatorial regions (mostly Cameroon), it shows weaker contributions in most Sahelian areas similar to ENSO and AMO (Fig. 8f). Although possible uncertainties in the MERRA data over the region can also limit its capability in quantifying accurately the impacts of IOD on TWS, warranting future consideration of inherent uncertainties in the data, Diatta and Fink (2014) observed statistically significant negative correlations of IOD (-0.30 and -0.23) with rainfall indices at West and Central Sahel areas. Some studies based on model experiments and observations (see, Nicholson, 2013, and the references therein) have argued that both Indian Ocean warming and SST gradients in the Indian Ocean have considerable influence on Sahel rainfall. Even though large scale climatological shifts in the Indian Ocean SST are

also the fall-out of other processes of oceanic variability such as the ENSO (Farnsworth et al., 2011), the observed drying trend in the West Sahel from the 1950s to the 1990s was attributed to the warming trend in the Indian Ocean (see, Bader and Latif, 2003). Put together, this may imply a possible signature of IOD in West Africa's rainfall, in addition to the well known connection of AMO and ENSO with rainfall variability in the region (see, e.g., Martin and Thorncroft, 2014; Diatta and Fink, 2014; Nicholson, 2013; Paeth et al., 2012; Panthou et al., 2012; Nicholson et al., 2000). So far, this study speculates that the mechanism of influence of IOD on TWS in the region may be at best complementary. Based on the result shown in Fig. 8 and our hypothesis that indices related rainfall impact on catchment storage (especially the Gulf of Guinea countries), it is our view, that these indices of climate variability in the region, collectively impact on the leading orthogonal modes of TWS (IC1, Fig. 7) in the region, exacerbating its variability. Apparently, MERRA-TWS over the Guinea Coast countries show statistically significant associations with all climate modes probably due to its long term records, which makes it possible to extract complete oscillations in each climate index unlike the GRACE data.

TWS over Gabon and some parts of the Congo basin have relatively strong semi-annual patterns (Fig. 6). The presence of strong seasonal rainfall in Guinea Coast countries, Gabon and much of the Congo basin also accounts for the observed TWS modes (Fig. 7) and semi annual amplitudes (Fig. 6). While non-symmetric meteorological signals (e.g., a strong rise in summer rainfall anomalies) may also create considerable peaks in the hydrological time series (TWS), much of the equatorial regions (e.g., Congo, Gabon, etc.) have huge water fluxes (e.g., surface runoff) and vegetative cover that show strong sensitivity to rainfall conditions, SST anomalies and other perturbations of the nearby oceans. Given that the climate of Gabon is tropical in nature, with single wet season between October and May, leading to $200-250$ mm of rainfall (see, McSweeney et al., 2010), the strong semi annual amplitude of TWS (Fig. 6b) in this area may also be associated with multiple climate modes as shown in Fig. 8a-f. Such relationship however, may require further clarification as the records of GRACE observation increases.

Furthermore, ENSO shows a stronger association (especially over the Volta basin, which explains the strongest variability in TWS-24.9% (IC1, Fig. 7) with observed TWS changes (see Table 4). From all indications, apart from the observed amplitude of AMO TWS (i.e., using MERRA-TWS) (Fig. 8e), in much of the Guinea Coast countries, ENSO is more closely related to GRACE-TWS changes in the region. This is exemplified in the inter-annual fluctuations of TWS of the first three ICA modes, which jointly explained 52.8% of the total variability (i.e.,

IC1−IC3, Fig. 7) and showed a much higher association with ENSO (-0.4 and -0.3) compared to other climate modes (IOD and AMO). Using GRACE-derived TWS during the $2003-2010$ period, Phillips et al. (2012) observed that in tropical regions, ENSO was negatively correlated with TWS, consistent with our observed relationship of the leading TWS modes with ENSO (IC1, Fig. 7). In a recent study over West Africa where available water expressed in terms of net-precipitation ($1979-2010$) was analysed using wavelet coherence analysis, decreasing rate in available water was highly coupled to a low frequency modulating El-Niño (see, Andam-Akorful et al., 2017). Other remarkable footprints of these climate modes in the region are also documented. For example, in the Sahel, ENSO, AMO, and IOD were found to have strong association with precipitation at periodicity (Okonkwo, 2014). In a study analysing global trends and variability in soil moisture and drought characteristics, West Africa is one of the areas in the world where inter-annual and decadal variations in soil moisture are driven mainly by variabilities in ENSO and AMO (see, Sheffield and Wood, 2008). Considering the results in preceding sections (Figs. 3, 4, and 7), hydrological conditions of the Lake Volta, arguably have some remote links with ENSO events and aligns with earlier reports (e.g., Owusu et al., 2008). Since TWS change over the Volta basin is also significantly driven by variations in Lake Volta water levels, the influence of ENSO in the basin presumably exists. For example, even after removing the annual and semi-annual components of TWS, the amplitudes of TWS in late 2010 and 2012 periods in the vicinity of the Volta basin reached ~ 200 mm (i.e., jointly derived from the temporal/spatial patterns), coinciding with the strong La-Niña events of $2010-2011$ and $2011-2012$ (IC1, Fig. 7). Similarly, the hydrological drought of 2001/2002 in the Volta basin (e.g., Ndehedehe et al., 2016c; Bekoe and Logah, 2013) is also consistent with our observed spatio-temporal fluctuations of wet/dry conditions (IC2, Figs. 4 and 5). The hydrological drought during this period ($2001-2002$) resulted in one of the lowest negative anomalies (i.e., ~ -200 mm when jointly derived from the first ICA mode of Fig. 7) observed in GRACE-derived TWS in the Volta catchment since inception of GRACE observations. Although the observed drought of 2001/2002 in the region remains the general signature of climate variability rather than the influence of these specific climatic indices, it nonetheless, gives credence to our hypothesis that the impact of extreme rainfall fluctuations leads to increased or decreased catchment storage in the region.

Based on the premise that drought conditions are primarily the result of precipitation deficits, and can lead to reduced recharge of the soil column (Sheffield and Wood, 2008), then this assumption holds. On the contrary, catchment characteristics, land use change, changes in temperature, and other meteorological and ecological processes can interact in complex ways

that accentuates TWS variations in the region. For instance, during periods of precipitation deficits in Niger (Sahel region), an extensive network of well observations showed that groundwater levels and water table increased significantly due to land clearing and land use change (see, Favreau et al., 2009; Séguis et al., 2004; Leduc et al., 2001). Similar complex hydrological processes were reported for south-east Australia and south-west US (see, Scanlon et al., 2005; Allison et al., 1990). Although the influence of non-climatic factors (e.g., shrub removal) on hydrological changes remains unclear in central Texas (see, Wilcox, 2007), Cattle trampling and timber harvesting triggered an evolution of runoff regime in northern Mexico (see, Viramontes and Descroix, 2003), confirming the influence of human activities on hydrological changes. The Sahel is a semi-arid ecosystem and one would naturally expect water availability through rainfall and soil moisture as major hydrological indicators of ecosystem performance. But Seghieri et al. (2012) found that a decrease in temperature was the strongest predictor of both leafing and reproductive phenophases in the Sahel. Collectively, these are some indications that the impact of non-climate teleconnection factors on hydrological processes exists in the region, especially the Sahel and other semi-arid regions.

From the foregoing, nonetheless, our presumptive evidence, is that ENSO (i.e., depending on the phase) impacts more on TWS in West Africa and leads to strong changes in surface and sub-surface storage (i.e., at seasonal scales). The analyses in this study also show a strong presence of AMO TWS in the coastal West African countries and much of the regions below latitude 10°N (Fig. 8e). As noted over the Sahel, positive phase of AMO coincides with above-normal rainfall or wet conditions and the negative phase with drought conditions (IC1, Figs. 3 and 4). This could be an evidence that corroborates the strong presence of AMO-driven TWS in the region as shown in Fig. 8e. However, considering the rather weak correlations of these climate modes with the localised time series of the leading GRACE-TWS modes, there might be indication that other low frequency climate oscillations combined with the influence of atmospheric circulations may be related to TWS over the region. The study is cautious in this regard but affirms that as the records of GRACE observation increases, this physical mechanisms and others can be investigated much more systematically with clarity and simplicity.

6. Conclusions

The presence of climate teleconnection (i.e., ENSO, AMO, and IOD) induced TWS changes derived from GRACE and MERRA over West Africa was studied using a suite of statistical techniques. The leading spatio-temporal modes of TWS and extreme rainfall anomalies (wet

and drought events) were identified and their possible relationship to climate teleconnections in the region were examined using correlation analysis. The results of the study are summarised as follows:

(i) The leading modes of SPI at 6 and 12 month aggregation indicating extreme drought/wet conditions coincided with extreme low/high amplitudes of TWS during the same period, giving credence to our hypothesis that the impact of extreme rainfall fluctuations leads to increased or decreased catchment storage in the region. While it is generally expected that large anomalies in rainfall are likely to generate low/high values of SPI (drought or wet conditions), leading to large anomalies in TWS (extreme low/high amplitudes), it is sometimes not usually the case for areas where water availability is also driven by temperature and in ecosystems where human activities (e.g., land clearing) have modified the land surface and soil characteristics. These scenarios, which result in complex hydrological processes (e.g., increasing water table during periods of strong precipitation deficits) have been highlighted in previous reports in the Sahel region and are few exceptions to the above argument. AMO and ENSO noticeably explains some of the variability in the observed SPI over the Sahel and the equatorial regions, suggesting that these teleconnections also play key roles in the characteristics of extreme climatic conditions in the region.

(ii) While ENSO appears to be more associated with TWS in the region and shows a statistically significant correlation with the observed temporal patterns of TWS, our analysis here also show a strong presence of AMO induced TWS in the coastal West African countries and much of the regions below latitude 10°N. The AMO has a wider footprint and sphere of influence on the region's TWS and suggests the important role of North Atlantic temperature in the region. Its association with temporal evolutions of SPI may have implications on TWS, especially in the semi-arid regions, though in complex ways, that requires further investigation. There are also statistically significant relationships between TWS and teleconnections (ENSO, AMO and IOD) in much of the Sahel region. Nonetheless, the contribution of the latter to TWS in the Sahel is considerably weak and maybe related to the rainfall structure of the region.

(iii) The impacts of IOD on the Western African hydrology appears to be unclear but shows statistically significant contribution to the long term MERRA-TWS for the countries along the coast and coincided with observed fluctuating drought conditions observed between 2005 and 2012 in eastern Guinea and Liberia. Global climate simulations in which IOD-like SST anomalies are imposed could help to clarify the role of IOD on the region's TWS and can be taken into consideration in future studies. Although this study confirmed the existence of

IOD-induced TWS in the region, which at best may be complimentary, TWS over much of West Africa and countries of the Congo basin are more likely to be influenced by ENSO and AMO events.

(iv) As some areas in the Sahel show strong AMO contributions to GRACE-TWS compared to the observed weak AMO-related MERRA-TWS, there are possibilities of false associations of GRACE-TWS with teleconnections (especially AMO) probably due to the limited time span of GRACE observations. However, the rather weak correlations of these climate modes with localised time series of GRACE-TWS, may also give the impression that other climate oscillations and atmospheric circulations could be associated with TWS changes in the region. The study is rather cautious in this regard but optimistic that as the records of GRACE observation increases with time, these physical mechanisms and others can be investigated much more systematically with clarity, simplicity, and very limited uncertainties. A robust analysis to help examine specific zones of global SSTs that impacts on TWS amplitudes over West Africa could provide more insights into the relationship between TWS and climate teleconnections and will be the subject of future considerations.

Acknowledgments

Christopher and Nathan are grateful to Curtin University for the funding through the CSIRS programme. Joseph is grateful for the financial support of the Japan Society of Promotion of Science for supporting his stay at Kyoto University (Japan) and the conducive working atmosphere provided by his host Prof Yoichi Fukuda (Department of Geophysics, Kyoto University, Japan). We also thank the Editor and the two anonymous reviewers for their very useful comments, which helped improved the manuscript. The Authors are grateful to CSR, NOAA, and NASA for the various data used in this study.

References

Adler, R. F., Huffman, G. J., Chang, A., Ferraro, R., Xie, P.-P., Janowiak, J., Rudolf, B., Schneider, U., Curtis, S., Bolvin, D., Gruber, A., Susskind, J., Arkin, P., and Nelkin, E. (2003). The version-2 Global Precipitation Climatology Project (GPCP) monthly precipitation analysis (1979Present). *Journal of Hydrometeorology*, 4(6):1147–1167. doi:10.1175/1525-7541(2003)004¡1147:TVGPCP¿2.0.CO;2.

Agutu, N., Awange, J., Zerihun, A., Ndehedehe, C., Kuhn, M., and Fukuda, Y. (2017). Assessing multi-satellite remote sensing, reanalysis, and land surface models' products in characterizing agricultural drought in East Africa. *Remote Sensing of Environment*, 194(0):287–302. doi:10.1016/j.rse.2017.03.041.

Ahmed, M., Sultan, M., J.Wahr, and Yan, E. (2014). The use of GRACE data to monitor natural and anthropogenic induced variations in water availability across Africa. *Earth Science Reviews*, 136:289–300. doi:10.1016/j.earscirev.2014.05.009.

Aires, F., Rossow, W. B., and ChéDin, A. (2002). Rotation of EOFs by the independent component analysis: Toward a solution of the mixing problem in the decomposition of geophysical time series. *Journal of the Atmospheric Sciences*, 59:111–123. doi:10.1175/1520-0469(2002)059¡0111:ROEBTI¿2.0.CO;2.

Ali, A. and Lebel, T. (2009). The Sahelian standardized rainfall index revisited. *International Journal Of Climatology*, 29:1705–1714. doi:10.1002/joc.1832.

Allison, G., Cook, P., Barnett, S., Walker, G., Jolly, I., and Hughes, M. (1990). Land clearance and river salinisation in the western Murray Basin, Australia. *Journal of Hydrology*, 119(1):1 – 20. doi:10.1016/0022-1694(90)90030-2.

Amani, A., Thomas, J., and Abou, M. N. (2007). Climate change adaptation and water resources management in West Africa. Synthesis report WRITESHOP. *UNESCO*. Retrieved from: www.nlcap./net/032135.070920.NCAP. Accessed 15th April 2014.

Andam-Akorful, S., Ferreira, V., Ndehedehe, C. E., and Quaye-Ballard, J. (2017). An investigation into the freshwater variability in West Africa during $1979 - 2010$. *International Journal of Climatology*. doi:10.1002/joc.5006.

Awange, J., Khandu, Schumacher, M., Forootan, E., and Heck, B. (2016). Exploring hydro-meteorological drought patterns over the Greater Horn of Africa (1979-2014) us-

841 ing remote sensing and reanalysis products. *Advances in Water Resources*, 94:45 – 59.
842 doi:10.1016/j.advwatres.2016.04.005.

843 Bader, J. and Latif, M. (2003). The impact of decadal-scale Indian Ocean sea surface tem-
844 perature anomalies on Sahelian rainfall and the North Atlantic Oscillation. *Geophysical*
845 *Research Letters*, 30(22). doi:10.1029/2003GL018426.

846 Bader, J. and Latif, M. (2011). The 1983 drought in the West Sahel: A case study. *Climate*
847 *Dynamics*, 36(3-4):463–472. doi:10.1007/s00382-009-0700-y.

848 Barry, B., Obuobie, E., Andreini, M., Andah, W., and Pluquet, M. (2005). Comprehen-
849 sive assessment of water management in agriculture: Comparative study of river basin
850 development and management. *International Water Management Institute*. Retrieved
851 from:www.iwmi.cgiar.org/assessment, Accessed 11 November, 2015.

852 Bekoe, E. O. and Logah, F. Y. (2013). The impact of droughts and climate change on electricity
853 generation in Ghana. *Environmental Sciences*, 1(1):13–24.

854 Boening, C., Willis, J. K., Landerer, F. W., Nerem, R. S., and Fasullo, J. (2012). The
855 2011 La Nia: So strong, the oceans fell. *Geophysical Research Letters*, 39(19):L19602.
856 doi:10.1029/2012GL053055.

857 Boergens, E., Rangelova, E., Sideris, M. G., and Kusche, J. (2014). Assessment of the
858 capabilities of the temporal and spatiotemporal ICA method for geophysical signal sep-
859 aration in GRACE data. *Journal of Geophysical Research Solid Earth*, 119:4429–4447,.
860 doi:10.1002/2013JB010452.

861 Boone, A., Decharme, B., Guichard, F., Rosnay, P. D., Balsamo, G., Belaars, A., Chopin,
862 F., Orgeval, T., Polcher, J., Delire, C., Ducharne, A., Gascoin, S., Grippa, M., Jarlan, L.,
863 Kergoat, L., Mougin, E., Gusev, Y., Nasonova, O., Harris, P., Taylor, C., Norgaard, A.,
864 Sandholt, I., Ottle, C., Poccard-Leclercq, I., Saux-Picart, S., and Xue, Y. (2009). The
865 AMMA Land Surface Model Intercomparison Project (ALMIP). *Bulletin of American Me-*
866 *teorological Society*, 90(12):1865–1880. doi:10.1175/2009BAMS27/86.1.

867 Cai, W., Santoso, A., Wang, G., Weller, E., Wu, L., Ashok, K., Masumoto, Y., and Yamagata,
868 T. (2014). Increased frequency of extreme indian ocean dipole events due to greenhouse
869 warming. *Nature*, 510(7504):254–258. doi:10.1038/nature13327,.

Cardoso, J.-F. (1991). Super-symmetric decomposition of the fourth-order cumulant tensor, blind identification of more sources than sensors. Retrieved from:http://perso.telecom-paristech.fr/ cardoso/Papers.PDF/icassp91.pdf. Accessed 15 January 2016.

Cardoso, J. F. (1999). High-Order contrasts for Independent Component Analysis. *Neural Computation*, 11:157–192.

Cardoso, J. F. and Souloumiac, A. (1993). Blind beamforming for non-gaussian signals. *IEE Proceedings*, 140(6):362–370.

Chen, J. L. and Wilson, C. R. (2008). Low degree gravity changes from GRACE, Earth rotation, geophysical models, and satellite laser ranging. *Journal of Geophysical Research: Solid Earth*, 113(B6). doi:10.1029/2007JB005397.

Cheng, M. K., Tapley, B. D., and Ries, J. C. (2013). Deceleration in the Earth's oblateness. *Journal of Geophysical Research*, 118:1–8. doi:10.1002/jgrb.50058.

Chylek, P., Klett, J. D., Dubey, M. K., and Hengartner, N. (2016). The role of Atlantic Multi-decadal Oscillation in the global mean temperature variability. *Climate Dynamics*, 47(9):3271–3279.

Common, P. (1994). Independent component analysis, A new concept? *Signal Processing*, 36:287–314.

Conway, D., Persechino, A., Ardoin-Bardin, S., Hamandawana, H., Dieulin, C., and Mahé, G. (2009). Rainfall and water resources variability in Sub-Saharan Africa during the twentieth century. *Journal of Hydrometeorology*, 10(1):41–59. doi:10.1175/2008JHM1004.1.

Dai, A., Qian, T., Trenberth, K. E., and Milliman, J. D. (2009). Changes in continental freshwater discharge from 1948 to 2004. *Journal of Climate*, 22(10):2773–2792. doi:10.1175/2008JCLI2592.1.

Descroix, L., Mahé, G., Lebel, T., Favreau, G., Galle, S., Gautier, E., Olivry, J.-C., Albergel, J., Amogu, O., Cappelaere, B., Dessouassi, R., Diedhiou, A., Breton, E. L., Mamadou, I., and Sighomnou, D. (2009). Spatio-temporal variability of hydrological regimes around the boundaries between Sahelian and Sudanian areas of West Africa: A synthesis. *Journal of Hydrology*, 375(12):90–102. doi:10.1016/j.jhydrol.2008.12.012.

Diatta, S. and Fink, A. H. (2014). Statistical relationship between remote climate indices and West African monsoon variability. *International Journal of Climatology*, 34(12):3348–3367. doi:0.1002/joc.3912.

Dong, L., Shimada, J., Kagabu, M., and Fu, C. (2015). Teleconnection and climatic oscillation in aquifer water level inKumamoto plain, Japan. *Hydrological Processes*, 29(7):1687–1703. doi:10.1002/hyp.10291.

Druyan, L. M. (2011). Studies of 21st-century precipitation trends over West Africa. *International Journal of Climatology*, 31(10):1415–1424. doi:10.1002/joc.2180.

FAO (1983). Integrating crops and livestock in West Africa. *Food and Agriculture Organization Of The United Nations*. Retrieved from:www.fao.org/docrep/004/x6543e/X6543E00. Accessed 10 May, 2015.

Farahmand, A. and AghaKouchak, A. (2015). A generalized framework for deriving nonparametric standardized drought indicators. *Advances in Water Resources*, (76):140–145. doi:/10.1016/j.advwatres.2014.11.012.

Farnsworth, A., White, E., Williams, C. J., Black, E., and Kniveton, D. R. (2011). *Understanding the Large Scale Driving Mechanisms of Rainfall Variability over Central Africa, In African Climate and Climate Change: Physical, Social and Political Perspectives*, pages 101–122. Springer Netherlands, Dordrecht. doi:10.1007/978-90-481-3842-5_5.

Favreau, G., Cappelaere, B., Massuel, S., Leblanc, M., Boucher, M., Boulain, N., and Leduc, C. (2009). Land clearing, climate variability, and water resources increase in semiarid southwest Niger: a review. *Water Resources Research*, 45:W00A16. doi:10.1029/2007WR006785.

Forootan, E., Awange, J., Kusche, J., Heck, B., and Eicker, A. (2012). Independent patterns of water mass anomalies over Australia from satellite data and models. *Remote Sensing of Environment*, 124:427–443.

Forootan, E., Kusche, J., Loth, I., Schuh, W. D., Eicker, A., Awange, J., Longuevergne, L., Diekkruger, B., and Shum, M. S. C. K. (2014). Multivariate prediction of total water storage changes over West Africa from multi-satellite data. *Surveys in Geophysics*, 35(4):913–940. doi:10.1007/s10712-014-9292-0.

Frappart, F., Ramillien, G., Leblanc, M., Tweed, S. O., Bonnet, M.-P., and Maisongrande, P. (2011). An independent component analysis filtering approach for estimating continental hydrology in the GRACE gravity data. *Remote Sensing of Environment*, 115(1):187 – 204. doi:doi.org/10.1016/j.rse.2010.08.017.

Frappart, F., Ramillien, G., Maisongrande, P., and Bonnet, M.-P. (2010). Denoising satellite

gravity signals by independent component analysis. *Geoscience and Remote Sensing Letters, IEEE*, 7(3):421–425. doi:10.1109/LGRS.2009.2037837.

Giannini, A., Biasutti, M., Held, I. M., and Sobel, A. H. (2008). A global perspective on African climate. *Climate Change*, 90(7):359–383. doi:10.1007/s10584-008-9396-y.

Giannini, A., Saravanan, R., and Chang, P. (2003). Oceanic forcing of Sahel rainfall on interannual to decadal time scales. *Science*, 302(5647):1027–1030. doi:10.1126/science.1089357.

Grippa, M., Kergoat, L., Frappart, F., Araud, Q., Boone, A., de Rosnay, P., Lemoine, J. M., Gascoin, S., Balsamo, G., Ottl, C., Decharme, B., Saux-Picart, S., and Ramillien, G. (2011). Land water storage variability over West Africa estimated by Gravity Recovery and Climate Experiment (GRACE) and land surface models. *Water Resources Research*, 47(5):W05549. doi:10.1029/2009wr008856.

Hao, Z. and AghaKouchak, A. (2014). A nonparametric multivariate multi-index drought monitoring framework. *Journal of Hydrometeorology*, 15(1):89–101. doi:10.1175/JHM-D-12-0160.1.

Hayes, M. J., Svoboda, M. D., Wilhite, D. A., and Vanyarkho, O. V. (1999). Monitoring the 1996 drought using the standardized precipitation index. *Bulletin of the American Meteorological Society*, 80:429–438. doi:10.1175/1520-0477(1999)080¡0429:MTDUTS¿2.0.CO;2.

Henry, C., Allen, D. M., and Huang, J. (2011). Groundwater storage variability and annual recharge using well-hydrograph and GRACE satellite data. *Hydrogeology Journal*, 19:741–755. doi:10.1007/s10040-011-0724-3.

Hinderer, J., de Linage, C., Boya, J.-P., Gegout, P., Masson, F., Rogister, Y., Amalvict, M., Pfeffer, J., Littel, F., Luck, B., Bayerb, R., Champollion, C., Collard, P., Moigne, N. L., Diamentc, M., Deroussi, S., de Viron, O., Biancale, R., Lemoine, J.-M., Bonvalot, S., Gabalda, G., Bock, O., Genthon, P., Boucher, M., Favreau, G., Sguis, L., Delclaux, F., Cappelaere, B., Oi, M., Descloitresh, M., Galleh, S., Laurent, J.-P., Legchenko, A., and Bouink, M.-N. (2009). The GHYRAF (Gravity and Hydrology in Africa) experiment: Description and first results. *Journal of Geodynamics*, 48:172–181. doi:10.1016/j.jog.2009.09.014.

Hodson, D. L. R., Sutton, R. T., Cassou, C., Keenlyside, N., Okumura, Y., and Zhou, T. (2010). Climate impacts of recent multidecadal changes in atlantic ocean sea surface temperature: a multimodel comparison. *Climate Dynamics*, 34(7):1041–1058. doi:10.1007/s00382-009-0571-2.

962 Hua, W., Zhou, L., Chen, H., Nicholson, S. E., Raghavendra, A., and Jiang, Y. (2016). Possible
963 causes of the Central Equatorial African long-term drought. *Environmental Research Letters*,
964 11(12):124002. doi:10.1088/1748-9326/11/12/124002.

965 Huffman, G. J., Adler, R. F., Bolvin, D. T., and Gu, G. (2009). Improving the global
966 precipitation record: GPCP Version 2.1. *Geophysical Research Letters*, 36(17):L17808.
967 doi:10.1029/2009GL040000.

968 Hurkmans, R., Troch, P. A., Uijlenhoet, R., Torfs, P., and Durcik, M. (2009). Effects of climate
969 variability on water storage in the Colorado River Basin. *Journal Of Hydrometeorology*,
970 10:1257–1270. doi:10.1175/2009JHM1133.1.

971 Ilin, A., Valpola, H., and Oja, E. (2005). Semiblind source separation of climate data detects el
972 nino as the component with the highest interannual variability. In *Proceedings. 2005 IEEE*
973 *International Joint Conference on Neural Networks, 2005.*, volume 3, pages 1722–1727.
974 doi:10.1109/IJCNN.2005.1556139.

975 Joly, M. and Voldoire, A. (2010). Role of the Gulf of Guinea in the inter-annual variability of the
976 West African monsoon: what do we learn from CMIP3 coupled simulations? *International*
977 *Journal of Climatology*, 30(12):1843–1856. doi:10.1002/joc.2026.

978 Kennedy, A. M., Garen, D. C., and Koch, R. W. (2009). The association between climate tele-
979 connection indices and Upper Klamath seasonal streamflow: Trans-niño index. *Hydrological*
980 *Processes*, 23(7):973–984. doi:10.1002/hyp.7200.

981 Kusche, J., Schmidt, R., Petrovic, S., and Rietbroek, R. (2009). Decorrelated GRACE time-
982 variable gravity solutions by GFZ, and their validation using a hydrological model. *Journal*
983 *of Geodesy*, 83(10):903–913. doi:10.1007/s00190-009-0308-3.

984 Lebel, T. and Ali, A. (2009). A physical basis for the interannual variability of rain-
985 fall in the Sahel. *Quarterly Journal Of The Royal Meteorological Society*, 375(1-2):5264.
986 doi:10.1016/j.jhydrol.2008.11.030.

987 Leduc, C., Favreau, G., and Schroeter, P. (2001). Long-term rise in a Sahelian water-table:
988 the continental terminal in south-west Niger. *Journal of Hydrology*, 243(1–2):43 – 54.
989 doi:10.1016/S0022-1694(00)00403-0.

990 Li, B. and Rodell, M. (2015). Evaluation of a model-based groundwater drought indicator in
991 the conterminous U.S. . *Journal of Hydrology*, 526:78 – 88. doi:10.1016/j.jhydrol.2014.09.027.

992 Li, K., Coe, M., Ramankutty, N., and Jong, R. D. (2007). Modeling the hydrological
993 impact of land-use change in West Africa. *Journal of Hydrology*, 337(3–4):258 – 268.
994 doi:10.1016/j.jhydrol.2007.01.038.

995 Lloyd-Hughes, B. (2012). A spatio-temporal structure-based approach to drought characteri-
996 sation. *International Journal of Climatology*, 32(3):406–418. doi:10.1002/joc.2280.

997 Losada, T., Rodríguez-Fonseca, B., Janicot, S., Gervois, S., Chauvin, F., and Ruti, P. (2010).
998 A multi-model approach to the Atlantic Equatorial mode: impact on the West African
999 monsoon. *Climate Dynamics*, 35(1):29–43. doi:10.1007/s00382-009-0625-5.

1000 MacDonald, A. M., Bonsor, H. C., Dochartaigh, B. E. O., and Taylor, R. G. (2012). Quan-
1001 titative maps of groundwater resources in Africa. *Environmental Research Letters*, 7.
1002 doi:10.1088/1748-9326/7/2/024009.

1003 Malhi, Y. and Wright, J. (2004). Spatial patterns and recent trends in the climate of tropical
1004 rainforest regions. *Philosophical Transactions of the Royal Society of London*, 359:311329.
1005 doi:10.1098/rstb.2003.1433.

1006 Martin, E. R. and Thorncroft, C. D. (2014). The impact of AMO on the West African
1007 monsoon annual cycle. *Quarterly Journal of the Royal Meteorological Society*, 140:31–46.
1008 doi:10.1002/qj.2107.

1009 Masih, I., Maskey, S., Mussá, F. E. F., and Trambauer, P. (2014). A review of droughts on
1010 the African continent: a geospatial and long-term perspective. *Hydrology and Earth System*
1011 *Sciences*, 18(9):3635–3649. doi:10.5194/hess-18-3635-2014.

1012 McKee, T. B., Doeskin, N. J., and Kieist, J. (1993). The relationship of
1013 drought frequency and duration to time scales. *Conference on Applied Climatol-*
1014 *ogy, American Meteorological Society,Boston, Massachusetts*, pages 179–184. Retrieved
1015 from:www.ccc.atmos.colostate.edu/relationshipofdroughtfrequency.pdf. Accessed 27 June,
1016 2014.

1017 McSweeney, C., New, M., Lizcano, G., and Lu, X. (2010). The UNDP climate change country
1018 profiles improving the accessibility of observed and projected climate information for studies
1019 of climate change in developing countries. *Bulletin of the American Meteorological Society*,
1020 91(2):157–166. doi:10.1175/2009BAMS2826.1.

1021 Mishra, A. K. and Singh, V. P. (2010). A review of drought concepts. *Journal of Hydrology*,
1022 391:202–216. doi:10.1016/j.jhydrol.2010.07.012.

Mohino, E., Janicot, S., and Bader, J. (2011). Sahel rainfall and decadal to multi-decadal sea surface temperature variability. *Climate Dynamics*, 37:419–440. doi:10.1007/s00382-010-0867-2.

Molion, L. C. B. and Lucio, P. S. (2013). A note on Pacific Decadal Oscillation, El Nino Southern Oscillation, Atlantic Multidecadal Oscillation and the Intertropical Front in Sahel, Africa. *Atmospheric and Climate Sciences*, 3:269–274. doi:10.4236/acs.2013.33028.

Molua, E. L. and Lambi, C. M. (2006). Climate, hydrology and water resources in Cameroon. *CEEPA, Discussion Paper*, (33). Retrieved from:http://www.ceepa.co.za/uploads/files/CDP33.pdf. Accessed 6 August, 2014.

Moore, P. and Williams, S. D. P. (2014). Integration of altimetry lake lavels and GRACE gravimetry over Africa: Inferences for terrestrial water storage change 2003-2011. *Water Resources Research*, 50:9696–9720. doi:10.1002/2014WR015506.

Ndehedehe, C., Awange, J., Agutu, N., Kuhn, M., and Heck, B. (2016a). Understanding changes in terrestrial water storage over West Africa between 2002 and 2014. *Advances in Water Resources*, 88:211–230. doi:10.1016/j.advwatres.2015.12.009.

Ndehedehe, C. E., Agutu, N. O., Okwuashi, O. H., and Ferreira, V. G. (2016b). Spatio-temporal variability of droughts and terrestrial water storage over Lake Chad Basin using independent component analysis. *Journal of Hydrology*, 540:106– 128. doi:10.1016/j.jhydrol.2016.05.068.

Ndehedehe, C. E., Awange, J., Kuhn, M., Agutu, N., and Fukuda, Y. (2017). Analysis of hydrological variability over the Volta river basin using in-situ data and satellite observations. *Journal of Hydrology: Regional studies*, 12:88–110. doi:10.1016/j.ejrh.2017.04.005.

Ndehedehe, C. E., Awange, J. L., Corner, R., Kuhn, M., and Okwuashi, O. (2016c). On the potentials of multiple climate variables in assessing the spatio-temporal characteristics of hydrological droughts over the Volta Basin. *Science of the Total Environment*, 557-558:819–837. doi:10.1016/j.scitotenv.2016.03.004.

Nicholson, S. (2013). The West African Sahel: a review of recent studies on the rainfall regime and its interannual variability. *ISRN Meteorology*, 2013(453521):1–32. doi:10.1155/2013/453521.

Nicholson, S. and Grist, J. (2001). A conceptual model for understanding rainfall variability

in the West African Sahel on interannual and interdecadal timescales. *International Journal Of Climatology*, 21:1733–1757. doi:10.1002/joc.648.

Nicholson, S. E., Some, B., and Kone, B. (2000). An Analysis of Recent Rainfall Conditions in West Africa, Including the Rainy Seasons of the 1997 El Niño and the 1998 La Nia Years. *Journal of Climate*, 13(14):2628–2640. doi:10.1175/1520-0442(2000)013¡2628:AAORRC¿2.0.CO;2.

Oguntunde, P. G. and Abiodun, B. J. (2013). The impact of climate change on the Niger River Basin hydroclimatology. *Climate Dynamics*, 40(1-2):81–94. doi:10.1007/s00382-012-1498-6.

Okonkwo, C. (2014). An Advanced Review of the Relationships between Sahel Precipitation and Climate Indices: A Wavelet Approach. *International Journal of Atmospheric Sciences*, 2014:11. doi:10.1155/2014/759067.

Owusu, K., Waylen, P., and Qiu, Y. (2008). Changing rainfall inputs in the Volta basin: implications for water sharing in Ghana. *GeoJournal*, 71(4):201–210. doi:10.1007/s10708-008-9156-6.

Paeth, H., Fink, A., Pohle, S., Keis, F., Machel, H., and Samimi, C. (2012). Meteorological characteristics and potential causes of the 2007 flood in sub-Saharan Africa. *International Journal of Climatology*, 31:1908–1926. doi:10.1002/Joc.2199.

Panthou, G., Vischel, T., Lebel, T., Blanchet, J., Quantin, G., and Ali, A. (2012). Extreme rainfall in West Africa: A regional modeling. *Water Resources Research*, 48(8):W08501. doi:10.1029/2012wr012052.

Phillips, T., Nerem, R. S., Fox-Kemper, B., Famiglietti, J. S., and Rajagopalan, B. (2012). The influence of ENSO on global terrestrial water storage using GRACE. *Geophysical Research Letters*, 39:L16705. doi:10.1029/2012GL052495, 2012.

Polo, I., Rodríguez-Fonseca, B., Losada, T., and García-Serrano, J. (2008). Tropical atlantic variability modes (19792002). part i: Time-evolving sst modes related to West African rainfall. *Journal of Climate*, 21(24):6457–6475. doi:10.1175/2008JCLI2607.1.

Reason, C. J. C. and Rouault, M. (2006). Sea surface temperature variability in the tropical southeast Atlantic Ocean and West African rainfall. *Geophysical Research Letters*, 33(21):L21705. 10.1029/2006GL027145.

Redelsperger, J.-L. and Lebel, T. (2009). Surface processes and water cycle in West Africa, studied from the AMMA-CATCH observing system. *Journal of Hydrology*, 375(1-2):1–2. doi:10.1016/j.jhydrol.2009.08.017.

Redelsperger, J.-L., Thorncraft, C. D., Diedhiou, A., Lebel, T., Parker, D. J., and Polcher, J. (2006). African monsoon multidisciplinary analysis. An international research project and field campaign. *Bulletin of the American Meteorological Society*, 87(12):1739–1746. doi:10.1175/BAMS-87-12-1739.

Reichle, R. H., Koster, R. D., Lannoy, G. J. M. D., Forman, B. A., Liu, Q., Mahanama, S. P. P., and Tour, A. (2011). Assessment and enhancement of MERRA land surface hydrology estimates. *Journal of Climate*, 24(24):6322–6338. doi:10.1175/JCLI-D-10-05033.1.

Rienecker, M. M., Suarez, M. J., Gelaro, R., Todling, R., Bacmeister, J., Liu, E., Bosilovich, M. G., Schubert, S. D., Takacs, L., Kim, G.-K., Bloom, S., Chen, J., Collins, D., Conaty, A., da Silva, A., Gu, W., Joiner, J., Koster, R. D., Lucchesi, R., Molod, A., Owens, T., Pawson, S., Pegion, P., Redder, C. R., Reichle, R., Robertson, F. R., Ruddick, A. G., Sienkiewicz, M., and Woollen, J. (2011). MERRA: NASA's modern-era retrospective analysis for research and applications. *Journal of Climate*, 24(14):3624–3648. doi:10.1175/JCLI-D-11-00015.1.

Rodríguez-Fonseca, B., Janicot, S., Mohino, E., Losada, T., Bader, J., Caminade, C., Chauvin, F., Fontaine, B., García-Serrano, J., Gervois, S., Joly, M., Polo, I., Ruti, P., Roucou, P., and Voldoire, A. (2011). Interannual and decadal SST-forced responses of the West African monsoon. *Atmospheric Science Letters*, 12:67–74. doi:10.1002/asl.308.

Saji, N. H., Goswami, B. N., Vinayachandran, P. N., and Yamagata, T. (1999). A dipole mode in the tropical Indian Ocean. *Nature*, 401:360–363.

Sanogo, S., Fink, A. H., Omotosho, J. A., Ba, A., Redl, R., and Ermert, V. (2015). Spatio-temporal characteristics of the recent rainfall recovery in West Africa. *International Journal of Climatology*, 35(15):4589–4605. doi:10.1002/joc.4309.

Scanlon, B. R., Keese, K. E., Flint, A. L., Flint, L. E., Gaye, C. B., Edmunds, W. M., and Simmers, I. (2006). Global synthesis of groundwater recharge in semiarid and arid regions. *Hydrological Processes*, 20(15):3335–3370. doi:10.1002/hyp.6335.

Scanlon, B. R., Reedy, R. C., Stonestrom, D. A., Prudic, D. E., and Dennehy, K. F. (2005). Impact of land use and land cover change on groundwater recharge and quality in the southwestern US. *Global Change Biology*, 11(10):1577–1593. doi:10.1111/j.1365-2486.2005.01026.x.

Seghieri, J., Carreau, J., Boulain, N., De Rosnay, P., Arjounin, M., and Timouk, F. (2012). Is water availability really the main environmental factor controlling the phenology of woody vegetation in the central Sahel ? *Plant Ecology*, 213(5):861–870. doi:10.1007/s11258-012-0048-y.

Séguis, L., Cappelaere, B., Milsi, G., Peugeot, C., Massuel, S., and Favreau, G. (2004). Simulated impacts of climate change and land-clearing on runoff from a small Sahelian catchment. *Hydrological Processes*, 18(17):3401–3413. doi:10.1002/hyp.1503.

Seo, K.-W., Wilson, C. R., Chen, J., and Waliser, D. E. (2008). GRACE's spatial aliasing error. *Geophysical Journal International*, 172(1):41–48.

Shahin, M. (2008). Hydrology and water resources of Africa. *Water Science and Technology Library*, (41). Kluwer Academic Publishers, Dordrecht, The Netherlands.

Sheffield, J. and Wood, E. F. (2008). Global trends and variability in soil moisture and drought characteristics, 1950–2000, from observation-driven simulations of the terrestrial hydrologic cycle. *Journal of Climate*, 21(3):432–458. doi:10.1175/2007JCLI1822.1.

Shukla, S. and Wood, A. W. (2008). Use of a standardized runoff index for characterizing hydrologic drought. *Geophysical Research Letters*, 35(2):L02405. 10.1029/2007GL032487.

Swenson, S., Chambers, D., and Wahr, J. (2008). Estimating geocenter variations from a combination of GRACE and ocean model output. *Geophysical Research Letters*, 31:1–4. doi:10.1029/ 2004GL019920.

Tapley, B., Bettadpur, S., Watkins, M., and Reigber, C. (2004). The Gravity Recovery and Climate Experiment: Mission overview and early results. *Geophysical Research Letters*, 31:1–4. doi:10.1029/ 2004GL019920.

Theis, F. J., Gruber, P., Keck, I. R., Meyer-bse, A., and Lang, E. W. (2005). Spatiotemporal blind source separation using double-sided approximate joint diagonalization. In *In Proc. EUSIPCO 2005*.

Trenberth, K. E. and Shea, D. J. (2006). Atlantic hurricanes and natural variability in 2005. *Geophysical Research Letters*, 33(12):L12704. doi:10.1029/2006GL026894.

USAID (2013). 2013 World population data sheet. *United States Agency International Development*. Retrieved from:www.prb.org. Accessed 2nd August 2014.

Viramontes, D. and Descroix, L. (2003). Changes in the surface water hydrologic characteristics of an endoreic basin of northern Mexico from 1970 to 1998. *Hydrological Processes*, 17(7):1291–1306. doi:10.1002/hyp.1285.

Wahr, J., Molenaar, M., and Bryan, F. (1998). Time variability of the Earth's gravity field: Hydrological and oceanic effects and their possible detection using GRACE. *Journal of Geophysical Research-Solid Earth*, 103(B12):30205–30229. doi:10.1029/98jb02844.

Westra, S., Brown, C., Lall, U., Koch, I., and Sharma, A. (2010). Interpreting variability in global SST data using independent component analysis and principal component analysis. *International Journal of Climatology*, 30(3):333–346. doi:10.1002/joc.1888.

Wilcox, B. P. (2007). Does rangeland degradation have implications for global streamflow? *Hydrological Processes*, 21(21):2961–2964. doi:10.1002/hyp.6856.

Wouters, B., Bonin, J. A., Chambers, D. P., Riva, R. E. M., Sasgen, I., and Wahr, J. (2014). GRACE, time-varying gravity, Earth system dynamics and climate change. *Reports on Progress in Physics*, 77(11):116801. doi:10.1088/0034-4885/77/11/116801.

Wu, M.-L. C., Reale, O., and Schubert, S. D. (2013). A characterization of Africaneasterly waves on $2.5-6$-day and $6-9$-day time scales. *Journal of Climate*, 26(18):6750–6774. doi:10.1175/JCLI-D-12-00336.1.

Yin, X., Gruber, A., and Arkin, P. (2004). Comparison of the GPCP and CMAP merged gaugesatellite monthly precipitation products for the period 19792001. *Journal of Hydrometeorology*, 5(6):1207–1222. doi10.1175/JHM-392.1.

Zhang, R. and Delworth, T. L. (2006). Impact of Atlantic multidecadal oscillations on India/Sahel rainfall and Atlantic hurricanes. *Geophysical Research Letters*, 33(17):L17712. doi:10.1029/2006GL026267.

Ziehe, A. (2005). Blind source separation based on joint diagonalization of matrices with applications in biomedical signal processing. *PhD thesis,Universitat Potsdam*. Retrieved from:http://en.youscribe.com/catalogue/reports-and-theses/knowledge/blind-source-separation-based-on-joint-diagonalization-of-matrices-1424347. Accessed 15 May 2015.